Global warming will largely increase waste treatment CH_4 emissions in Chinese Megacities: insight from the first city scale CH_4 concentration observation network in Hangzhou city, China

Cheng Hu[1,2], Junqing Zhang[1], Bing Qi[3,4*], Rongguang Du[3]*, Xiaofei Xu[4], Haoyu Xiong[5], Huili Liu[1], Xinyue Ai[1], Yiyi Peng[1], Wei Xiao[2]

[1] College of Biology and the Environment, Joint Center for sustainable Forestry in Southern China, Nanjing Forestry University, Nanjing 210037, China

[2] Collaborative Innovation Center on Forecast and Evaluation of Meteorological Disasters (CIC-FEMD), Nanjing University of Information Science & Technology, Nanjing, China

[3] Hangzhou meteorological bureau, Hangzhou 310051, China

[4] Zhejiang Lin'an Atmospheric Background National Observation and Research Station, Hangzhou 311300, China

[5] College of Environment, Zhejiang University of Technology, Hangzhou 311300, China

*Corresponding authors: Bing Qi (bill_129@sina.com), Rongguang Du (drg1998@163.com).

To be submitted to: *ACP*

Abstract:

Atmospheric CH_4 is the second largest anthropogenic contributor to global warming, however its emissions, components, spatial-temporal variations and projected changes still remain large uncertainty from city to national scales. CH_4 emissions from waste treatment (including solid waste landfills, solid waste incineration and sewage) account for even >50% of total anthropogenic CH_4 emissions at city scale, and considering the high sensitivity of CH_4 emission factors (EFs) to temperature for the biological processes-based sources as waste treatment, large bias will be caused in estimating future CH_4 emissions under different global warming scenarios. Furthermore, the relationships between temperature and waste treatment CH_4 emissions were only conducted in a few site-specific studies and lack the representativity for whole city, which contains various biophysical conditions and shows heterogeneous distribution. These above factors cause the evaluation of city scale CH_4 emissions (especially from waste treatments) and projected changes still remain unexplored. Here we conduct the first tower-based CH_4 observation network with three sites in Hangzhou city, which is located in developed Yangtze River Delta (YRD) area and ranks as one of the largest megacities in China. We found the *a priori* total annual anthropogenic CH_4 emissions and emission from waste treatment were overestimated by 36.0% and 47.1% in Hangzhou city, respectively. But total emission in larger region as Zhejiang province or YRD area was only slightly underestimated by 7.0%. Emissions from waste treatment showed obvious seasonal patterns following air temperature. By using the constructed linear relationship between monthly waste treatment CH_4 emissions and air temperature, we find the waste treatment EFs will increase by 38%~50% with temperature increases by 10^{o}C. Together with projected temperature changes from four climate change scenarios, the global warming induced EFs in Hangzhou city will increase at the rates of 2.2%, 1.2%, 0.7% and 0.5% per decade for RCP8.5, RCP6.0, RCP4.5 and RCP2.6 scenarios, respectively. And the EFs will finally increase by 17.6%, 9.6%, 5.6%, and 4.0% at the end of this century. Additionally, the derived relative changes in China also showed high heterogeneity and indicates large uncertainty in projecting future national total CH_4 emissions. Hence, we strongly suggest the temperature-dependent EFs and the positive feedback between global warming and CH_4 emissions should be considered in future CH_4 emission projections and climate change models.

Keyword: CH_4 emissions, waste treatment, observation network, global warming

1. Introduction

As the second largest anthropogenic greenhouse gas, the reduction of CH_4 emission is considered as an effective way to mitigate future climate change at short timescales (Henne et al., 2016; Lin et al., 2021). Accurate estimation of CH_4 emissions from its main sources are the basis of policy making. However, recent studies find there still remain large uncertainties for its total emissions, components, spatial-temporal variations and projected changes at city scale especially for megacities in China (USPA 2013; Cai et al., 2018; Lin et al., 2021). CH_4 emission from waste treatment (mainly including sewage and solid waste by landfills and incineration) ranked as the world's third largest anthropogenic source after fuel exploitation and livestock, and was responsible for ~13% of global anthropogenic CH_4 emissions of 371 (±26) Tg a^{-1} (Lu et al., 2021). It also ranked as the fourth largest anthropogenic source in China, the biggest anthropogenic CH_4 emitting country, and accounted for ~14% of national total anthropogenic emissions of 65 (±22) Tg a^{-1} (Saunois et al., 2020; Lu et al., 2021; Chen et al., 2022). Furthermore, its contribution is even larger than 50% at city scale especially for megacities, where both active and closed household waste (including landfills and waste water systems) are located and found as super emitters (Williams et al., 2022; Maasakkers et al., 2022). A large number of Chinese landfills were mainly constructed at the suburban more than 5-10 years ago, and with the urban area expanding in recent decades, the locations of many landfills are now in urban scope (Zhejiang Statistical Yearbook 2018-2019). Besides, the decreasing area of agricultural sector (rice paddies and husbandry) in megacities also makes their emissions ignorable when compared with waste treatment. Therefore, accurate quantification of CH_4 emissions from waste treatment in urban area becomes increasing important.

Although some progress has been made in measuring site scale CH_4 emissions from waste treatment, the estimated emissions still show large discrepancies due to many factors as the amount of waste and its composition, meteorological conditions as temperature, water content, atmospheric pressure and proportion between landfills and incineration, degradable organic carbon ratio, CH_4 oxidation efficiency, landfill gas collection (Masuda et al., 2018; Cai et al., 2018; Zhao et al., 2019; Hua et al., 2022; Bian et al., 2022; Maasakkers et al., 2022; Kissas et al., 2022).

Furthermore, CH_4 emissions from sewage and landfills are a microbial process especially from methanogens, its EFs are highly sensitive to temperature. These available studies were mainly conducted at some specific sites with measured EFs largely varied (Du et al., 2017; 2018; Cai et al., 2014; 2018; Zhao et al., 2019; NBSC, 2015; Wang et al., 2015; Florentino et al., 2010; Tolaymat et al., 2010; Hua et al., 2022). The lack and discrepancies of detailed information for all the above factors and their uncertainties have led to considerable bias in estimating CH_4 emissions for most-to-date inventories (Höglund-Isaksson, 2012; USEPA et al., 2013; Cai et al., 2018; Lin et al., 2021; Maasakkers et al., 2022).

China, the largest anthropogenic CH_4 emission and developing country, is supposed to increase its emissions because of projected rapid economic development, urbanization and generated waste (Cai et al., 2018). The increase of waste treatment emissions in east China was also found as the second largest sector in driving national total anthropogenic CH_4 emissions since 2000 (Lin et al., 2021). Besides, the mitigation potential of waste treatment in developing countries is thought four times of developed countries (USEPA, 2013). Therefore, mitigating CH_4 emissions from waste treatment in China is a robust and cost-effective way to reducing national total anthropogenic greenhouse gas emissions.

Many previous studies have estimated the waste treatment CH_4 emissions for China by both "bottom-up" and "top-down" approaches, with results varied by 2.5-fold from 4.3 to 10.4 Tg CH_4 yr^{-1}, and accounted for 8.1%~24.2% of national total anthropogenic CH_4 emissions (USEPA 2013; Peng et al., 2016; Miller et al., 2019; Lin et al., 2021; Lu et al., 2021; Chen et al., 2022). For these "bottom-up" approach, the high uncertainties were directly attributed to omission of many small point sources and discrepancies of observed site-specific EFs, which varied largely by climate and management technology (Zhao et al., 2019; Hua et al., 2022). As were found in previous studies that the most commonly used EDGAR (The Emission Database for Global Atmospheric Research) inventory always used IPCC recommended default EF values as 15.0% (Höglund-Isaksson, 2012; Lin et al., 2021; Bian et al., 2022), but this value was around 5-7 times of EFs used in China by Zhang and Chen et al. (2014). A recent study by comparing waste treatment CH_4 emissions among

different inventories also reported that the EDGAR v5.0 and CEDS (Community Emissions Data System) inventories were 21~153% higher than other inventories, and EDGAR v5.0 tended to assign more emissions in urban area especially for provincial capitals. In addition, emission from wastewater was found overestimated by higher emission factor or chemical oxygen demand (Peng et al., 2016; Lin et al., 2021).

And for the "top-down" atmospheric inversion approach, a few studies constrained anthropogenic sources including waste treatment, where the most widely used concentrations were satellite observations (Miller et al., 2019; Lu et al., 2021; Chen et al., 2022). The satellite retrieval owns advantage of easy data access and global coverage. But as already noted, the emission constraint results are highly dependent on availability of observed concentrations, which are largely influenced by weather conditions and cloud coverage. As was illustrated in a nearly published study by Chen et al. (2022), although the numbers of grid cell ($0.25^{o} \times 0.3125^{o}$) based year-round satellite observations were more than 1000 in north China, the available numbers were less than 10 (and even without any observations) in most part of central, west, east and south China. Such sparse distribution of available data may not provide robust constraint on waste treatment emissions for some Chinese cities without enough observations, especially considering waste treatment is co-located with high population density megacities of developed area as east and south China. Furthermore, there should be large temperature induced monthly variations for waste treatment CH_4 emissions, but almost all satellite-based inversions were conducted at annual scale without seasonal variations. Besides, given the strong influence from atmospheric pressure on landfill CH_4 emissions, satellite observations are too sparse to be up-scaled to estimate annual total because satellite observations are almost conducted in clear-sky conditions and cannot represent atmospheric pressure and CH_4 emissions in cloudy or rainy days. There was only one recent study by using satellite observations and focused on urban waste treatment CH_4 emissions, it found annual CH_4 emissions from four cities were 1.4 to 2.6 times larger than inventories in India and Pakistan, where landfills contributed to 6~50% of total emissions and indicated large bias of our understanding of waste treatment CH_4 emissions (Maasakkers et al., 2022).

149 The tower-based atmospheric inversion approach, which is based on hourly atmospheric
150 concentration observations within planetary boundary layer, can be used independently to
151 constrain CH_4 emissions and its main components. Besides, compared with "bottom-up" approach,
152 this method can avoid using the factors that lead to large uncertainties of CH_4 emissions especially
153 from waste treatment. And to our best knowledge, there is few tower-based observation inversion
154 studies which focuses on waste treatment emissions at city scale or much larger regional scales
155 especially in China. Only one study in Los Angeles, U.S.A. used tower-based CH_4 concentration
156 and found the influence of landfill site closure on CH_4 emissions, which was not included in *a*
157 *priori* inventory (Yadav et al., 2019). Besides, the influences of global warming on city scale (or
158 higher regional scale) emissions were still unclear and have not been considered in future emission
159 projections (USEPA 2013; Cai et al., 2018). In general, previous studies which predicted future
160 waste treatment CH_4 emissions only used activity data changes, without considering climate
161 change on its EFs. Considering the potential high sensitivity of waste treatment CH_4 emissions on
162 the projected global warming, how will its emission change with increasing temperature is still
163 unknown, especially within megacities where more waste was generated and urban heat island
164 effect will lead to much stronger warming climate (Zhang et al., 2022).
165
166 Here, we established three tower-based CH_4 concentration observation sites in Hangzhou city, one
167 of the largest megacities in China. To our best knowledge, it's the first city scale tower-based CH_4
168 concentration observation network in China. We present our work on urban CH_4 emissions
169 inversion and aim to (1) constrain CH_4 emissions from waste treatment alongside total
170 anthropogenic emissions in Hangzhou city, (2) derive temperature sensitivity of waste treatment
171 CH_4 emissions at city scale and quantify the projected emission changes in future climate change
172 scenarios. One-year hourly CH_4 concentration observations from December 1st, 2020 to
173 November 30th, 2021 were combined with atmospheric transport model and Bayesian inversion
174 approach to constrain monthly CH_4 emission inventories. The constructed relationship between
175 monthly temperature and *posteriori* waste treatment CH_4 emissions will be used with future
176 temperature projection to quantify how will its EFs change in different global warming scenarios.
177

2. Materials and Method

2.1 Tower-based CH_4 observation network and supplementary materials

The Hangzhou city, which has a population of 12.2 million and area of 1.7×10^4 km^2 (core urban area of 8.3×10^3 km^2), is the capital of Zhejiang province and located in middle of east China (Figure 1a). As displayed in Figures S1-S2, the east China accounted for majority of national total population and waste treatment CH_4 emissions, and Hangzhou city ranked as the top 10 megacities in China with annual solid waste of around 5 million tons in 2021. The tower-based CH_4 concentration observation network includes three observation sites (Figure 1a-d), as (1) Hangzhou site (120.17° E, 30.23° N, 43.2 m a.s.l.), which is located in the core urban regions; (2) Linan site (119.72° E, 30.30° N, 138.6 m a.s.l.), regional background site with none obvious emission sources within 10 km radius; (3) Damingshan site (119.00° E, 30.03° N, 1485.0 m a.s.l.), which is built on the top of a 1500 m mountain and represents background from much more diluted regional emission signals. The distance is around 50 km between Hangzhou site and Linan site, and around 150 km between Hangzhou site and Damingshan site. These three sites represent obvious gradients from east of densely populated area (Figure 1c-d) and anthropogenic emissions to west of much weaker anthropogenic influence and background conditions. Based on the wind direction for three sites, there are not obvious difference of seasonal wind direction patterns among them. The prevailing wind direction from October to February was from the north, which changed to east from February to May and then changed to south during the monsoon in summer.

The air inlet heights are 25 m above ground for Hangzhou site, 53 m at Linan site and 10 m at Damingshan site, respectively. Atmospheric CH_4 concentrations at all three sites were continuously measured by cavity ring-down spectroscopy analyzer (model G2301 for Hangzhou site and G2401 for Linan site and Damingshan site; Picarro Inc., Sunnyvale, CA). To obtain high precision observations, two different standard gas was measured every 6 hours and a linear two-point fit was used to calibrate observations, with the precision and accuracy of 2 ppb and 1 ppb. More details of the observation and calibration systems were descripted in Fang et al., (2014; 2022). Note because of instrument issues at Damingshan site, there is some data gap in September and October, 2021. In general, 99.4%, 99.0%, 79.3% of hourly CH_4 observations were available in

the whole year observation period for Hangzhou site, Linan site and Damingshan site, respectively. Meteorological observations at Hangzhou meteorological station were used to evaluate simulated meteorological fields, including air temperature at 2 m (T_{2m}), relative humidity (RH), downward solar radiation (S↓), and wind speed (WS) at 10 m height.

Note some previous studies of city scale greenhouse gas concentration observation networks chose sites at the edge of urban borders as background in emission inversion system (i.e. Indianapolis, U.S.A., Miles et al., (2017); Los Angeles, U.S.A., Verhulst et al., (2017); Washington, DC-Baltimore, U.S.A., Lopez-Coto et al., (2020); Paris, France, Lian et al., (2021)), but we chose to use five CH_4 background sites as the potential background to be selected including UUM, TAP, YRO, YON and WLG site (Figure 1a), which were much further than the observations at Damingshan site. This strategy is based on following three reasons: (1) our footprint domain is much larger than Hangzhou city and these five sites are also located close to the edge of model domain; (2) CH_4 concentrations within Hangzhou city will be influenced by seasonal varied monsoon and the monthly varied wind directions will lead to obvious changes of CH_4 background than only at Damingshan site; (3) our model setups can partition CH_4 enhancements from within Hangzhou city and other regions.

The projected climate data from four RCP (Representative Concentration Pathway) scenarios (RCP8.5, RCP6.0, RCP4.5 and RCP2.6) by MRI-CGCM3 model were downloaded from World Data Center for Climate (WDCC, https://www.wdc-climate.de/ui/), where annual air temperature at 2m was used from years 2021 to 2100. The most recent population density data for Hangzhou city is for the year of 2019 and was downloaded from Chinese national resource and environmental science and data center (http://www.resdc.cn/DOI),2017.DOI:10.12078/2017121101).

2.2 WRF-STILT model setup

The WRF-STILT (WRF: Weather Research and Forecasting, version 4.2.2, and STILT: Stochastic Time-Inverted Lagrangian Transport) model will be used to simulate hourly footprint and CH_4 enhancement, see more details in Hu et al. (2019; 2021). Domain setups are displayed in Figure 1a,

with the outer nested domain (Domian-1, 27 km×27 km grid resolution) covers eastern and central China, and the inner domain (Domain-2, 9 km×9 km grid resolution) covers YRD area. The physical schemes used in the WRF model are the same as in our previous studies for YRD domain (Hu et al., 2019; 2021). The simulated CH_4 concentration is the sum of background and enhancement, where the enhancement is calculated by multiplying all CH_4 flux with hourly footprint that represents the sensitivity of the concentration changes to its regional sources/sinks with spatial resolution of $0.1^o \times 0.1^o$. To better quantify CH_4 components at each site, CH_4 enhancements from different regions and sources are also tracked and separately simulated. Besides, we should note the CH_4 background is important in simulating CH_4 concentrations and atmospheric inversion. We will choose CH_4 background from the five background sites based on monthly footprint as discussed in Section 3.1.

The most recent inventory of Emission Database for Global Atmospheric Research (EDGAR v6.0), which has 20 categories, and WetCHARTs ensemble mean were used as the *a priori* anthropogenic and natural CH_4 emissions. We should note there are many CH_4 inventories for some developed regions and countries (i.e. France, U.S.A., Germany) with high spatial resolutions, the reasons to choose EDGAR as *a priori* anthropogenic emissions are: (1) for all available CH_4 inventories that covered China, the spatial resolution of EDGAR ($0.1^o \times 0.1^o$) is the highest, and it provide most up-to date results; (2) most of previous studies that constrain emissions by atmospheric inversion studies also chosed EDGAR, and our results can be directly compared with previous studies; (3) the preliminary simulation of CH_4 concentrations showed generally good performance with observations, indicating its spatial distributions in Hangzhou city has relatively small bias even with potential large bias for magnitude, which will be constrained by our atmospheric inversion method.

The main sources in Hangzhou city include SWD_LDF (solid waste landfills), WWT (waste water handling), SWD_INC (solid waste incineration), PRO (all processes related to fuel exploitation from coal, oil, and natural gas), RCO (energy for buildings, mainly containing nature gas escape from household use) and AGS (agricultural soils). We found emissions from SWD_LDF, WWT

and SWD_INC were simply assigned in the same locations in EDGAR inventory, and hence combined them as waste treatment. For the CH_4 emissions from wetland, we used WetCHARTs ensemble mean with spatial resolution of 0.5° at monthly average (Bloom et al., 2017). Considering WetCHARTs treat rice paddies (main source as AGS) as one wetland type, AGS in EDGAR was excluded and we assume WetCHARTs represent all wetland CH_4 emissions as natural wetland and rice paddies.

2.3 **Bayesian inversion framework**

The Scale Factor Bayesian inversion (SFBI) approach was applied to interpret the atmospheric CH_4 concentration (or enhancement) variations in terms of quantitative constraint on all CH_4 sources. The relationship between observed and simulated CH_4 concentrations (or enhancement) can be expressed as follows in Equation 1:

$$y = \mathrm{K}\Gamma + \varepsilon \qquad (1)$$

Where y is the observed CH_4 concentration (or enhancement), K corresponds to simulated enhancements from all categories, Γ is the state vector to be optimized and consists of *posteriori* SFs for corresponding categories in K, and ε is the observing system error.

The optimal solution to derive *posteriori* SFs is to minimize a cost function J(Γ), which represents the mismatch between CH_4 observations and simulations and the mismatch between *posteriori* and *a priori* SFs (Miller et al., 2008; Griffis et al., 2017). The cost function J(Γ) can be expressed as:

$$\mathrm{J}(\Gamma) = \frac{1}{2}\left[(y-\mathrm{K}\Gamma)^T S_e^{-1}(y-K\Gamma) + (\Gamma-\Gamma_{\mathrm{a}})^T S_a^{-1}(\Gamma-\Gamma_{\mathrm{a}})\right] \qquad (2)$$

where S_e and S_a are the constructed error covariance matrices for observations and the *a priori* values, and S_e consists of measurement and model errors. Here each element in *a priori* SFs Γ_a is treated as 1. Therefore, the solution for obtaining the *posteriori* SFs is to solve $\nabla_\Gamma J(\Gamma) = 0$, and is given by,

$$\Gamma_{\mathrm{post}} = (K^T S_e^{-1} K + S_a^{-1})^{-1}(K^T S_e^{-1} y + S_a^{-1}\Gamma_{\mathrm{a}}) \qquad (3)$$

In the Bayesian inversion framework, we first need to give an estimate of the error covariance matrices and the state vector for the *a priori* and observational data. And following our previous studies conducted in East China (Hu et al., 2019; 2022). The uncertainty of 10%, 13% and 20%

were assigned to the measurement errors (S_{obs}), the finite number of particles (500) released in the STILT model ($S_{particles}$) and uncertainty in meteorological fields (S_{met}), respectively.

Although previous study derived uncertainty of CH_4 from waste treatment and other categories, which varied between 30% and 50%, these uncertainties were calculated mainly from activity data and EFs at the country scale on annual average (Solazzo et al. 2021). We should also note CH_4 emission uncertainty will largely increase with study region decreasing, as stated above the relative difference among different inventories can reach to 150%. Considering the disaggregation of spatial distributions and temporal variations, CH_4 emission uncertainties can be much larger at urban and monthly scales. To provide robust constraint on CH_4 emissions in our study, we used three cases of *a priori* uncertainties combinations for different emissions in Bayesian inversion as: (1) the first case use three elements as wetland, waste treatment and the rest anthropogenic sources, considering the larger seasonality of waste treatment, the uncertainties of 300% was used for waste treatment and 200% for other categories, (2) the second case have more detailed categories as wetland, waste treatment, fuel exploitation, energy for building, and the rest anthropogenic sources, where the *a priori* uncertainty of 200% was used for each categories, (3) the third case has the same categories as case 1 but use a different *a priori* uncertainty for waste treatment of 200%. The averages of all three cases are used as final *posteriori* SFs and the largest difference between each of three cases are used as uncertainty.

3. Results

3.1 Atmospheric CH_4 observations

We first displayed the hourly CH_4 concentrations from our three tower-based sites and smoothed background at five sites by CCGCRV fitting method (Thoning et al., 1989) in Figure 2a. It's obvious the hourly observations at three towers showed similar temporal variations but with different amplitude. Observations at Hangzhou site displayed variations between 2000 ppb and 2800 ppb, and were much larger than both Linan site and Damingshan site. Their monthly averages were also compared in Figure 2b, and results showed the monthly CH_4 varied between lowest 2106.3 ppb in July and highest 2225.0 ppb in September (annual mean of 2159.9 ppb) at Hangzhou site, lowest 2023.3 ppb in July and highest 2132.0 ppb in September (annual mean of

2086.7 ppb) at Linan site, the lowest 1955.5 ppb in July and without observations in September at Damingshan site (annual mean of 2013.4±(3) ppb, where the uncertainty is calculated when assuming the missing data in September and October varied between August and November), respectively. The similar trends among three sites can be explained that they were dominated by similar atmospheric transport processes, such as synoptic process (i.e. monsoon) and seasonal changing wind direction as summarized above. But their surrounding emission sources are highly different, implying the emissions of Hangzhou site should be much larger than Linan and Damingshan sites.

Because the CH_4 background is important in concentration simulation and emission inversion, we also compared CH_4 background between five sites, where the annual averages at TAP, YON, RYO, WLG and UUM were 1989.8 ppb, 1850.1 ppb, 1982.7 ppb, 1973.4 ppb and 1984.2 ppb, respectively. We found the difference were generally within 20 ppb among TAP, RYO, WLG and UUM sites (Figure 2), but there is large difference between YON site and other four sites from May to August, which can reach to around 100 ppb. Note YON site is located in the south of East China Sea (Figure 1a), it can be influenced by monsoon with clean air flows from the South China Sea, which have much less CH_4 sources compared to air flows from Asian land area. The CH_4 background at TAP site appeared slightly higher than other four sites because TAP site is located in coast of South Korea and can be more easily polluted by anthropogenic emissions. Considering above large spatial difference between CH_4 background sites, monthly air flows and source footprint will be used to identify backgrounds for our observation network, with details discussed in Supplementary Material (Section S2, Figure S3 and Table S1).

3.2 Concentration footprint and *a priori* emissions

To illustrate the potential source regions of three sites, the annual averages of simulated footprints for each site are displayed in Figure 3a-c. Results show their footprint distributions were quite similar because of close distance, but we also notice there were obvious difference for footprint strength (i.e. the area covered by red color) with Hangzhou site > Linan site > Damingshan site. The reason why footprint at Damingshan site is the lowest is that observations was conducted at

1500 m height, which was not easy to receive emission signals within boundary layer heights. Besides, the Hangzhou site is located in the core urban area of Hangzhou city, and it will show significant diurnal variation in PBLH, especially have higher nighttime PBLH caused by anthropogenic heat and high buildings than grassland/farmland dominated Linan site and Damingshan site. Hence more air particles can retain within PBLH and generated stronger footprint.

The *a priori* EDGAR CH_4 emissions for total anthropogenic categories, waste treatment and its proportions are further illustrated in Figure 3d-f. It shown significant gradients from higher emissions in east to lower emissions in the west, which is consistent with our three tower-based observations. And the CH_4 emissions for waste treatment displayed similar spatial distributions with urban land use and population density (Figure 1c-d), besides, waste treatment seems emitted CH_4 by area sources instead of point sources as waste treatment super plants. Although a few previous studies found limitations of EDGAR inventory to capture CH_4 emission patterns in some urban areas (Pak et al., 2021), here considering the fact that locations of landfills, which is the largest anthropogenic CH_4 emitter in Hangzhou city, are very close to the core urban area and in high consistence with EDGAR, hence we believe the spatial patterns of EDGAR in study region can be reliable. We should note the Chinese government constructed waste separation station in each city with density of one station for per 150~200 households (around 450~800 people), which can emit lots of methane caused by daily biomass waste as area sources (Tian et al., 2022). These above analyses also imply Hangzhou site can observe higher emissions from both waste treatment and total anthropogenic emissions, which will be discussed and quantified later.

3.3 Simulation of CH_4 concentrations and its components for three sites

Comparisons between observed and simulated daily CH_4 concentration averages are displayed in Figure 4a-c and hourly concentrations in Figure S4 for three sites. First, the hourly simulations in Figure S4 showed high consistence when only comparing the temporal patterns with observations, indicating good performance of model transport simulations as confirmed in Figure S5 for evaluating meteorological fields. But the relative variations display obvious difference among

three sites for daily averages in Figure 4a-c. The mean bias (MB), root mean squared error (RMSE), and correlation coefficient (R) between daily observations and *a priori* simulations were 64.1 ppb, 129.2 ppb and 0.44, respectively, for Hangzhou site; and were -6.0 ppb, 57.1 ppb, 0.50 for Linan site, 36.2 ppb, 55.6 ppb, 0.54 for Damingshan site. As for Hangzhou site, simulated CH_4 concentrations show obvious overestimation from October to April, and the overestimation was also found at Damingshan site. We found the simulations at Linan site shows overall good agreement with observation, but still with slight overestimation from January to April and underestimation from May to September. Considering the source area contributions for three sites are different, these difference among three sites indicated the bias in CH_4 emission largely varied from Hangzhou city to larger regional scale.

To further quantify detailed contributions from different regions and categories to each tower site, CH_4 enhancements from different categories and source area were also simulated separately for three sites. As displayed in Figure 4d-e, the simulated *a priori* total enhancements at Hangzhou site, Linan site, and Damingshan site were 244.3 ppb, 100.8, and 69.0 ppb, respectively. We also found contributions by waste treatments dominated the total enhancements but with obvious difference among three sites, which varied from the highest 64.2% at Hangzhou site to the lowest 41.4% at Damingshan site. We further calculated anthropogenic contributions from Hangzhou city (excluding wetland because of coarser spatial resolution for Hangzhou city) and other provinces, which were 158.4 ppb at Hangzhou site, 30.7 ppb at Linan site, and 10.1 ppb at Damingshan site, respectively. And they accounted for 69.3%, 34.0%, and 16.9% of total anthropogenic enhancements at corresponding sites. These results indicate the CH_4 observations at Hangzhou site, which is located at the core urban region, was more influenced by local emissions (mainly for waste treatment and will be discussed later) and contain much higher enhancements than other two sites. The relative contributions from different regions also imply that the observations at Linan and Damingshan sites can present CH_4 emissions of much larger region as Zhejiang province or YRD area than Hangzhou city (Figure 4e).

The seasonal-averaged diurnal variations for both observations and simulations are also displayed

in Figure 5 for three sites. Although many previous studies only used daytime observations and simulations to evaluate *a priori* emissions bias and constrain emissions (Sargent et al., 2018; Hu et al., 2022), these studies were based on the assumption that the used diurnal scaling factors on *a priori* emissions are right (i.e. for anthropogenic CO_2), or the emissions do not have obvious diurnal variations (i.e. emissions from industries or manufacturing). Here as concluded above that the main CH_4 component in Hangzhou city was waste treatment (Figure 3f), which should be highly sensitive to temperature and indicates obvious diurnal and seasonal patterns (Mønster et al., 2019; Kumar et al., 2022). And its emissions will be overestimated if only use daytime emissions to represent daily averages. Further, we found high similarities of the diurnal variations between observations and simulations for three sites, but there are still some discrepancies especially that the observations at Linan site were generally higher than simulations from spring to autumn for both all-day and midday averages.

Hence, our preliminary conclusions were that the *a priori* CH_4 emissions were generally overestimated for Hangzhou city but underestimated in larger region as Zhejiang or YRD area. We also found simulations were higher than observations for all seasons at Damingshan site, and it can be explained by the high heterogeneity around Damingshan site, where elevations changed from 0 m to 1600 m within the site located grid cell of 9 km (~ 0.1°) as displayed in Figure 1b, and the mountain-valley wind, PBLH changes can only be resolved with much higher spatial resolutions as < 1km. Hence the use of coarse resolutions (i.e. 9 km in this study) at the mountainous regions will bring large bias in simulating concentration and emission inversion, as also recently found in China for CO_2 as "aggregation error" (Agustí-Panareda et al., 2019; Wang et al., 2022), so observations at Damingshan site will not be used in emission inversions in this study.

3.4 Constraint on anthropogenic CH_4 emissions

As were displayed in Figures 3f, 5a and concluded in Section 3.3, simulations by using *a priori* CH_4 emissions show obvious overestimations especially from October to April at Hangzhou site, and was also overestimated in winter and underestimated from spring to autumn at Linan site. Note this bias can be attributed to *a priori* emissions or meteorological simulations. Our previous

studies in YRD have evaluated the meteorological simulations by using the same physical parameterization schemes, which showed high consistence with observations (Hu et al., 2019; 2021; 2022; Huang et al., 2021). We also evaluated the meteorological simulations with observations and confirmed with good model performance (Figure S5). Note PBLH simulations are important in evaluating model performance, we did not have direct PBLH observations to evaluate model performance during the study period, but our previous study used the same physical and PBLH schemes as this study, which was conducted in Nanjing city in the same Domain 2 and vary close to Hangzhou city. This previous study found high consistence between observed and simulated PBLH in winter (Huang et al., 2021). Furthermore, we found there was not monthly variations in EDGAR v6.0 CH_4 emissions for waste treatment, which contributed 64.2% to annual CH_4 enhancement average and much higher in winter (Figure S6). The CH_4 emissions from waste treatment was a microbial process which should be affected by meteorological conditions especially by seasonal temperature changes. Hence our assumption was that bias in both its seasonality and annual average lead to large overestimation/underestimation in the simulated CH_4 concentration. Besides, bias in other anthropogenic emissions and wetland can also partly contributed to the bias of simulated CH_4 concentration.

To quantify the bias sources and constrain corresponding *a priori* emissions for Hangzhou city, we applied the scaling factor Bayesian inversion approach with three different cases as introduced in Method section. Instead of only using daytime CH_4 observations to constrain *a priori* emissions, we choose to use all-day hourly data at Hangzhou site to constrain emissions for Hangzhou city, which is based on following three reasons: (1) the enhancements contributed by Hangzhou city at Hangzhou site was 69.3%, and much larger than 34.0%, and 16.9% for Linan site and Damingshan site, respectively; (2) the waste treatment dominated anthropogenic CH_4 emissions in Hangzhou city, which is caused by biological process and should be temperature dependent. The observed temperature displays obvious diurnal variations by 20 ^{o}C, the use of only daytime observations without considering diurnal CH_4 emissions will bring significant bias when using derived daytime emissions to represent all-day averages. The annual averages of daytime and all-day average concentrations were 2112.4 and 2156.0 ppb at Hangzhou site, respectively, and

more comparisons between daytime and all-day average concentrations are displayed in Figure 5 for three sites; (3) previous study by using daytime observations were mainly conducted at regions dominated by industry or energy production, which have much smaller diurnal variations than waste treatment as stated above (Mønster et al., 2019; Kumar et al., 2022).

The derived monthly *posteriori* SFs for each emission source were displayed in Table 1 for Hangzhou city. Results showed the *posteriori* SFs for waste treatment were much smaller in winter and higher in summer, indicating obvious seasonality and the overestimation in winter was mainly contributed by waste treatment. The annual mean *posteriori* SFs for waste treatment varied between 0.50 and 0.56 in all three cases, illustrating overestimation at annual average for the *a priori* waste treatment emissions. Besides, the annual mean *posteriori* SFs varied between 0.87 and 0.94 for rest total anthropogenic categories (excluding agricultural soil), and were 0.97 for PRO (fuel exploitation) and 0.91 for RCO (energy for building), respectively; the annual mean *posteriori* SFs and were 1.05 and 1.05 for wetland (including agricultural soil and natural wetland). These *posteriori* SFs for the rest anthropogenic categories and wetland indicated much smaller bias than waste treatment. The monthly *posteriori* SFs for PRO and RCO also illustrated obvious seasonal variations, but were still smaller than the *a priori* seasonality in inventory (Figure S7).

To evaluate whether the *posteriori* SFs have significantly improved CH_4 emissions, we used these SFs to derive the *posteriori* emissions and re-simulated hourly concentrations in Figure 6 (and daily averages in Figure S8). Results showed the hourly overestimation by using *a priori* emissions was largely reduced by using *posteriori* emissions when compared with observations in Figure 6a-b, and the regression slope between daily averaged observations and simulations decreased from 1.51(±0.15) for *a priori* simulations to 0.85(±0.07) for *posteriori* simulations in Figure 6c. The mean bias (MB), root mean squared errors (RMSE), correlation coefficient (R) between daily observations and *a priori* simulations were 64.1 ppb, 129.2 ppb and 0.44, respectively, and these statistics changed to -22.2 ppb, 72.3 ppb and 0.58 for *posteriori* simulations. These results indicate the *posteriori* SFs obviously decreased the bias in *a priori* emissions and were much close to observations.

The comparisons of monthly CH_4 emissions between *a priori* and *posteriori* waste treatment and other anthropogenic sources (excluding agricultural soil) in Hangzhou city were displayed in Figures 7a and S7. For the *a priori* inventory, there is not seasonal variations for waste treatment with constant monthly emissions of 8.67×10^3t, and other anthropogenic sources showed seasonality with much higher in winter (i.e. 5.22×10^3t in January) than in summer (i.e. 3.06×10^3t in August). The seasonality in *a priori* EDGAR inventory was mainly dominated by RCO (Energy for buildings), with proportions to total anthropogenic emissions changed from the highest 22% in winter to lowest ~8% in summer. Such information indicates the *a priori* inventory assigned more leaks from natural gas distribution infrastructure in winter than in summer. As discussed above that the constant emissions from waste treatment should be wrong because of its large temperature sensitivity, and the observed monthly temperature difference between summer and winter was larger than 25°C in Hangzhou city. Here after the constraint by using observed concentration, the *posteriori* emissions for waste treatment showed obvious seasonality with highest value in July ($7.66 \pm 0.09 \times 10^3$ t) and lowest in February ($2.20 \pm 0.87 \times 10^3$ t). And the other anthropogenic emissions showed much smaller seasonality (highest in January of $4.18 \pm 0.69 \times 10^3$ t and lowest in August of $2.88 \pm 0.15 \times 10^3$ t) than *a priori* emissions. In general, the annual emission from waste treatment was 10.4×10^4 t in *a priori* EDGAR inventory and decreased to 5.5 (± 0.6) $\times 10^4$ t for the *posteriori* emissions by 47.1%. The *a priori* emissions from other anthropogenic sources was 4.5×10^4 t and only slightly decreased to 4.1 (± 0.3) $\times 10^4$ t for the *posteriori* emissions by 8.9%. The proportion of waste treatment to total anthropogenic emissions decreased from *a priori* 69.3% to *posteriori* 57.3%. To sum it up, the annual total anthropogenic CH_4 emissions (excluding agricultural soil) decreased from 15.0×10^4 t to 9.6 (± 0.9) $\times 10^4$ t, indicating overestimation of 36.0% in Hangzhou city for the *a priori* emissions.

However, as concluded above that the observations and simulations at Linan site, which represents much larger region as Zhejiang province or YRD area, illustrated slightly different results that CH_4 simulations were underestimated from spring to autumn and overestimated in winter (Figure 4b and Figure 5e-h). Here we used multiplicative scaling factor (MSF) method and observations at Linan site to derive SFs at seasonal scale (Sargent et al., 2018; He et al., 2020), where we used 10

ppb as the potential CH_4 background uncertainty in winter, spring and autumn, and 20 ppb in summer, see details in the Supplementary Material (Section S2). The derived *posteriori* SFs were 0.87 (±0.08), 1.07 (±0.11), 1.19 (±0.24), and 1.16 (±0.11) for winter, spring, summer, and autumn, respectively. It showed similar seasonal variations as found for Hangzhou city and was 1.07 (±0.14) of *a priori* anthropogenic emissions for the annual average. Our observations at Hangzhou site and Linan site together indicate the *a priori* emissions largely biased at both seasonal and annual scale, and the annual anthropogenic CH_4 emission was largely overestimated by 36.0% in Hangzhou city, but was underestimated by 7.0% in larger region as Zhejiang province or YRD area.

3.5 Temperature sensitivity of waste treatment CH_4 EFs and projected changes

Although the derived *posteriori* monthly SFs on waste treatment reflected changes on emissions, considering the monthly activity data does not have obvious monthly changes, these SFs can mainly reflect relative variations of monthly EFs and contain meteorological dominated changes especially for temperature. To evaluate the temperature sensitivity of its EFs, we first calculated the normalized monthly SFs by dividing monthly SFs by annual averages (Table S2), and quantified the relationship between observed T_{2m} and normalized SFs. The normalized SFs illustrated significant linear relationship with monthly T_{2m} (Figure 7b), where the slopes imply that normalized SFs (and EFs) will increase by 38%~50% with temperature increase by 10^{o}C at city scale.

We should note the precipitation, soil water content and atmospheric pressure can also have obvious influence on CH_4 emissions, and considering the fact that we have not conducted field measurement in landfills and landfills are usually covered by metal or plastic in China to avoid the spread of odor smell, hence reanalysis data cannot represent real soil water contents in these site scale landfills. Precipitation and atmospheric pressure showed obvious linear relationship with temperature as displayed in Figure S8. They displayed positive linear relationship between precipitation (affect water content) and T_{2m}, and negative linear relationship between monthly averaged atmospheric pressure and T_{2m}. We also found negative relationship between atmospheric

pressure and normalized SFs (Figure S8a). Considering air temperature always displays negative relationship with atmospheric pressure as warmer air temperature coincides with lighter air mas and lower atmospheric in summer, and colder air temperature coincides with heavier air mass and higher atmospheric pressure in winter. Hence, the temperature can be used to represent co-influence of both temperature and atmospheric pressure, and we only focus on the influence of temperature on CH_4 emissions and will add more supporting data in following studies.

Our findings for the high sensitivity of waste treatment CH_4 emissions to temperature also indicated dramatic increase with the projection of future global warming trends. We further derived the T_{2m} trends for four different RCP scenarios as RCP8.0, RCP6.0, RCP4.5 and RCP2.6 (Figure 8a), results showed T_{2m} will increase by 0.50°C, 0.28°C, 0.16°C, 0.10°C per decade for Hangzhou city, respectively. These different warming trends also indicate distinct temperature-dominated influence on future CH_4 EFs and emissions from waste treatment. We then used the slopes in Figure 7b and annual temperature from 2021 to 2100 to derive relative changes of EF in future 80 years, where observation year of 2021 was treated as the baseline year. As displayed in Figure 8b, the EFs in RCP8.5, RCP6.0, RCP4.5 and RCP2.6 scenarios will increase with the rates of 2.2%, 1.2%, 0.7% and 0.5% per decade, respectively. And CH_4 EFs for waste treatment will finally increase by 17.6%, 9.6%, 5.6%, and 4.0% at the end of this century.

The spatial distribution of T_{2m} trends for whole China were also displayed in Figure S10, which showed heterogeneous distributions across China for four global warming scenarios. Because east China is with high population density and the majority of national population (Figure S1), and owns the largest domestic garbage induced CH_4 emissions (Figure S2), these combined factors indicate considerable CH_4 emissions changes from waste treatment in such a temperature-sensitivity area. Considering the temperature sensitivity of waste treatment CH_4 EFs are caused by microbial process at the regional scales, it can represent general conditions of different cities or landfills. And if we assume the derived temperature sensitivity (increase by 44% with temperature increases by 10°C on average) is applicable for whole China especially for east China, the relative changes of waste treatment CH_4 EFs can be calculated by multiplying this

586 value with air temperature trends. And the spatial distributions of global warming induced EFs
587 changes at the end of this century are displayed Figure 9. For RCP2.6 scenario, EFs for waste
588 treatment will slightly increase by 4.0-6.5% in the north of east China and increase by 3.0-4.0% in
589 south of east China. The RCP6.0 also displayed heterogeneous changes in east China, with the
590 north of east China increase by 10.5-13.0% and south of east China increase by 9.0-10.5%.
591 Relative changes in RCP4.5 and RCP8.5 are more homogeneous for east China, which indicates
592 EFs will significantly increase by 5.0-7.5% and 17.5-19.5%, respectively. The largest changes will
593 occur in west China for RCP8.5 by >20.0%, but this area is with low population density and CH_4
594 emissions, and indicates ignorable effects of global warming (Figure S8). Finally, we should note
595 these derived relative changes are only caused by global warming, and the influence of activity
596 data, management technology and other factors is not considered and out of the scope of this
597 study.
598
599 **4 Discussions and implications**
600 Many previous studies have compared total CH_4 emissions and its components for different
601 inventories and bottom-up methods, which illustrated large uncertainty and bias at city scale and
602 these biases are much larger for waste treatment (Peng at al., 2016; Saunois et al., 2020; Lin et al.,
603 2021; Bian et al., 2022). A recent bottom-up research compared wastewater CH_4 EFs in China,
604 which largely varied by four-fold in different provinces and the uncertainty in the same province
605 were even two-fold larger than its average, implying considerable bias in recent understanding of
606 waste treatment EFs at regional scale (Hua et al., 2022). And for the national total emissions, it
607 varied between 5 and 15 Tg a^{-1} (Peng et al., 2016; EDGAR v6). There are also other atmospheric
608 inversion studies in estimating China's CH_4 emissions (Hopkins et al., 2016; Hu et al., 2019;
609 Huang et al., 2021; Miller et al., 2019; Lu el., 2021; Chen et al., 2022). These studies found large
610 bias of national-wide emissions for almost all inventories, which were mainly caused by fossil fuel
611 exploitation, agricultural sector (livestock and rice paddies) and waste treatment. For the
612 comparisons of waste treatment emissions, these satellite-based inversions also largely varied
613 between 6 and 9 Tg a^{-1} by 1.5-fold (Miller et al., 2019; Lu et al., 2021; Chen et al., 2022; Zhang et
614 al., 2022).

615 The above discrepancies between “bottom-up” and “top-down” approaches indicate large
616 uncertainty in understanding China’s national CH_4 emissions from waste treatment. And it is well
617 known the uncertainties increase from national scale to regional and cities, and also implying
618 considerable bias in city-scale emissions for inventories. But the atmospheric inversion approach
619 for city scale waste treatment, which can act as independent evaluation, is still rare not only for
620 China but also globally. To our best knowledge, there is only one recent atmospheric inversing
621 research focused on CH_4 emissions from city-scale waste treatment, which used satellite-based
622 observation to constrain emissions from four cities in India and Pakistan, that concluded
623 underestimation of landfills CH_4 emissions by 1.4 to 2.6 times for EDGAR inventory (Maasakkers
624 et al., 2022). In our study, we found annual waste CH_4 emissions were overestimated by 47.1% for
625 Hangzhou city, our findings are different with results in India and Pakistan. These differences
626 indicate bias of waste treatment CH_4 emissions considerably varied in different countries and
627 climate divisions. Our results highlight there is large knowledge gap in understanding its emission
628 mechanism and estimating urban waste treatment CH_4 emissions especially in China.
629
630 Different from other fossil-type sources that have much smaller monthly variations, waste
631 treatment is microbial process based and its EFs is highly sensitive to meteorological conditions
632 especially for temperature. These factors lead to obvious bias in waste treatment CH_4 emissions
633 not only for annual average but also for its seasonality. Besides, although there are a few studies
634 that aim to predict future CH_4 emissions from waste treatment, these studies were mainly based on
635 activity data changes without considering the EFs variations caused by future global warming
636 trends or only based on site-specific observations (USEPA 2013; Cai et al., 2018; Spokas et al.,
637 2021). For the mentioned three cited studies, USEPA (2013) and Cai et al. (2018) only predicted
638 emission change due to changes in activity data and management technology. And the CH_4
639 emissions for year of 2030 by Cai et al. (2018) was 23.5% lower than USEPA (2013) estimation,
640 which was caused by the consideration of new policies and low-carbon policy scenarios. And
641 Spokas et al. (2021) modeled the CH_4 emission changes with increasing air temperature, where
642 CH_4 emissions did not show obvious changes even with temperature increasing by ~5^{o}C at the end
643 of year 2100. To our best knowledge, there is not inventories that considered the temperature

induced changes on both its seasonal variations and annual trends. Hence, it's still unclear in all inventories how will EFs change with different global warming scenarios at city scale.

A few observation-based measurements were conducted for waste treatment but only at some specific sites with large discrepancies of EFs (Du et al., 2017; 2018; Cai et al., 2018; Zhao et al., 2019; NBSC, 2015; Wang et al., 2015; Florentino et al., 2010; Tolaymat et al., 2010; Cai et al., 2014; 2018). And only one of our previous study used year-round atmospheric CH_4 observations to constrain regional scale CH_4 emissions at Nanjing city in YRD area (Huang et al., 2021), it found much higher emissions of the landfilling waste in summer than in winter, and emissions in July was around four times in February. But there is not study that has quantified the temperature sensitivity of waste CH_4 emissions at city scale or much larger regional scales. These two studies in different cities confirmed temperature is the dominant factors that drive seasonal variations of waste treatment CH_4 emissions. Hence our study appears as the first one that estimated city scale waste treatment CH_4 emissions, its temperature sensitivity and projected changes in different global warming scenarios. Our findings for the large sensitivity on temperature indicate the monthly scaling factors should be considered to better simulate atmospheric CH_4 concentrations.

We also note that the predictions of future climate changes were mainly based on different emitting intensity of greenhouse gas, and CH_4 contributed around 20% of direct anthropogenic radiative forcing (Seto et al., 2014). The CH_4 emissions in different global warming scenarios were mainly calculated by predicting energy use data without consideration the changes of EFs. In this study, we found there should be large positive feedback between global warming and CH_4 emissions, especially in the RCP 8.0 scenario where global warming induced emissions will increase by 17.6%. Hence the projected emissions from waste treatments and other biological processes-based sources, together with positive feedback between temperature and their emissions are strongly suggested in future climate change models. Besides, it's well known the CH_4 concentration simulations are essential for modeling many air pollutions (i.e. O_3, NO_x, and CO) especially in stratosphere (Isaksen et al., 2011; Kaiho et al., 2013), and considering the waste treatment CH_4 emissions accounted for ~25% of total anthropogenic emissions (EDGAR v6.0) in

east China where severe air pollution frequently occurred, we also believe the coupling of temperature-dependent CH_4 emissions and the monthly scaling factors on CH_4 emissions can improve air pollution modeling in east China.

We should note that new technology and other meteorological variables can also influence waste treatment CH_4 emissions. The main reason to only use temperature in this study is that we only constrained the emissions at monthly scale in one year, and derived twelve datasets of *posteriori* CH_4 emissions. Besides, temperature is considered as the main factor in controlling monthly and annual variations of waste treatment CH_4 emissions, and can be used to represent co-influence of other meteorological parameters as atmospheric pressure. We will use multiple years' CH_4 concentration to quantify the influence of new technology and other meteorological variables on waste treatment CH_4 emissions in our following study, and we suggest other tracers (i.e. ethane, $^{14}CH_4$) are also important to separate CH_4 emissions from biological and fossil CH_4 emissions.

5 Conclusions

To better evaluate bias for city scale anthropogenic CH_4 emissions and understand the sensitivity of temperature on waste treatment CH_4 emissions, we conducted three tower-based atmospheric CH_4 observation network in Hangzhou city, which is located in developed YRD region and one of top 10 megacities in China. One-year hourly atmospheric CH_4 observations were presented from December 2020 to November 2021. We then applied a scaling factor Bayesian inversion method to constrain monthly anthropogenic CH_4 emissions and its components (especially for waste treatments) in Hangzhou city, and also used multiplicative scaling factor method for broader Zhejiang province and YRD area at seasonal scale.

To the best of our knowledge, our study is the first tower-based CH_4 observation network in China. We found obvious seasonal bias of simulated CH_4 concentrations at the core urban area of Hangzhou city, which was mainly caused by bias of waste treatment at both annual and monthly scales. The derived *posteriori* CH_4 emissions displayed significant seasonal variations with peak in summer and trough in winter which was mainly caused by waste treatment; the *a priori* annual

waste treatment CH_4 emission in Hangzhou city was 10.4×10^4 t and decreased to 5.5 (±0.6)$\times10^4$ t for the *posteriori* emissions by 47.1%. Besides, the total anthropogenic CH_4 emissions (excluding agricultural soil) decreased from 15.0×10^4 t to 9.6(±0.9)$\times10^4$ t, indicating overestimation of 36.0% for the whole year of 2021. Observations at Linan site imply that the annual CH_4 emissions was slightly underestimated by 7.0% in larger region as Zhejiang province or YRD area, which was different with Hangzhou city. Additionally, the *posteriori* monthly CH_4 emissions from waste treatment illustrated significant linear relationship with air temperature, with regression slopes indicating an increase of 38%~50% when temperature increases by 10^{o}C. Finally, we found the waste treatment CH_4 EFs for Hangzhou city will increase by 17.6%, 9.6%, 5.6%, and 4.0% at the end of this century for RCP8.0, RCP6.0, RCP4.5 and RCP2.6 scenarios, respectively. The derived relative changes for whole China also showed high heterogeneity and indicates large uncertainty in projecting future national total CH_4 emissions. This study is also the first one that mainly focuses on city scale temperature sensitivity of waste treatment CH_4 emissions from the perspective of atmospheric inversion approach. And based on above results, we strongly suggest the temperature-dependent EFs should be coupled in both recent CH_4 inventories and future CH_4 emission projections.

Data availability: The atmospheric CH_4 observations data can be requested from Cheng Hu and Bing Qi. STILT model is downloaded from http://www.stilt-model.org/, the EDGAR inventory is from https://edgar.jrc.ec.europa.eu/, and the projected climate data were downloaded from World Data Center for Climate (WDCC, https://www.wdc-climate.de/ui/).

Acknowledgement: Cheng Hu is supported by the National Natural Science foundation of China (grant no. 42105117) and Natural Science Foundation of Jiangsu Province (grant no. BK20200802). Wei Xiao is supported by the National Key R&D Program of China (grants 2020YFA0607501 & 2019YFA0607202). This work is also supported by Zhejiang Provincial Basic Public Welfare Research Project (LGF22D050004).

Author contribution: Cheng Hu and Bing Qi designed the study. Cheng Hu performed the model simulation, data analysis and wrote the paper; Bing Qi and Rongguang Du conducted CH_4 concentration observation and meteorological data collection, and all co-authors contributed to the data/figures preparation and analysis.

Declaration of competing interests: The authors declare that they have no conflict of interest.

References:

Agustí-Panareda, A., Diamantakis, M., Massart, S., Chevallier, F., Muñoz-Sabater, J., Barré, J., Curcoll, R., Engelen, R., Langerock, B., Law, R. M., Loh, Z., Morguí, J. A., Parrington, M., Peuch, V.-H., Ramonet, M., Roehl, C., Vermeulen, A. T., Warneke, T., and Wunch, D.: Modelling CO_2 weather – why horizontal resolution matters, Atmos. Chem. Phys., 19, 7347–7376, https://doi.org/10.5194/acp-19-7347-2019, 2019.

Bian R., Zhang T., Zhao F., et al. Greenhouse gas emissions from waste sectors in China during 2006–2019: Implications for carbon mitigation. Process. Saf. Environ., 161:488-497, 2022.

Bloom, A. A., Bowman, K. W., Lee, M., Turner, A. J., Schroeder, R., Worden, J. R., Weidner, R., McDonald, K. C., and Jacob, D. J.: A global wetland methane emissions and uncertainty dataset for atmospheric chemical transport models (WetCHARTs version 1.0), Geosci. Model Dev., 10, 2141–2156, https://doi.org/10.5194/gmd-10-2141-2017, 2017.

Cai, B., J. Liu, X. Zeng, D. Cao, L. Liu, Y. Zhou, Z. Zhang, Estimation of CH_4 emission from landfill in China based on point emission sources. Adv. Clim. Change Res. 5, 81–91, 2014.

Cai, B., Lou, Z., Wang, J., Geng, Y., Sarkis, J., Liu, J., and Gao, Q.: CH_4 mitigation potentials from China landfills and related environmental co-benefits, Sci. Adv., 4, eaar8400, https://doi.org/10.1126/sciadv.aar8400, 2018.

Chen, Z., Jacob, D. J., Nesser, H., Sulprizio, M. P., Lorente, A., Varon, D. J., Lu, X., Shen, L., Qu, Z., Penn, E., and Yu, X.: Methane emissions from China: a high-resolution inversion of TROPOMI satellite observations, Atmos. Chem. Phys., 22, 10809–10826, https://doi.org/10.5194/acp-22-10809-2022, 2022.

Du, M., Peng, C., Wang, X., Chen, H., Wang, M., and Zhu, Q.: Quantification of methane emissions from municipal solid waste landfills in China during the past decade, Renew. Sust. Energ. Rev., 78, 272–279, 2017.

Du, M., Zhu, Q., Wang, X., Li, P., Yang, B., Chen, H., Wang, M., Zhou, X., and Peng, C.: Estimates and predictions of methane emissions from wastewater in China from 2000 to 2020, Earths Future, 6, 252–263, 2018.

Fang S.X., R.G. Du, B. Qi. et al., Variation of carbon dioxide mole fraction at a typical urban area in the Yangtze River Delta, China. Atmos. Res, 265, 105884, 2022.

Florentino, Cruz., B. De La , and M. A. Barlaz ., Estimation of waste component-specific landfill decay rates using laboratory-scale decomposition data. Environ. Sci. Technol. 44, 4722–4728, 2010.

Griffis, T. J., Chen, Z., Baker, J. M., Wood, J. D., Millet, D. B., Lee, X., et al., Nitrous oxide emissions are enhanced in a warmer and wetter world. P. Natl. Acad. Sci. USA, 114(45), 12081–12085. https://doi.org/10.1073/pnas.1704552114, 2017.

He, J., Naik, V., Horowitz, L. W., Dlugokencky, E., and Thoning, K.: Investigation of the global methane budget over 1980–2017 using GFDL-AM4.1, Atmos. Chem. Phys., 2020, 20, 805–827, https://doi.org/10.5194/acp-20-805-2020.

Henne, S., Brunner, D., Oney, B., Leuenberger, M., Eugster, W., Bamberger, I., Meinhardt, F., Steinbacher, M., and

Emmenegger, L.: Validation of the Swiss methane emission inventory by atmospheric observations and inverse modelling, Atmos. Chem. Phys., 16, 3683–3710, https://doi.org/10.5194/acp-16- 3683-2016, 2016.

Hopkins, F. M., Kort, E. A., Bush, S. E., Ehleringer, J. R., Lai, C.-T., Blake, D. R., & Randerson, J. T. Spatial patterns and source attribution of urban methane in the Los Angeles Basin. J. Geophys. Res-Atmos., 121, 2490–2507, 2016.

Höglund-Isaksson, L.: Global anthropogenic methane emissions 2005–2030: technical mitigation potentials and costs, Atmos. Chem. Phys., 12, 9079–9096, https://doi.org/10.5194/acp-12- 9079-2012, 2012.

Hua, H., Jiang, S., Yuan, Z., Liu, X., Zhang, Y., & Cai, Z. Advancing greenhouse gas emission factors for municipal wastewater treatment plants in China. Environ. Pollut., 295, 118648. https://doi.org/10.1016/j.envpol.2021.118648, 2022.

Hu C, Griffis, T. J., Liu, S., Xiao, W., Hu, N., Huang, W., Yang, D., Lee, X., Anthropogenic methane emission and its partitioning for the Yangtze River Delta region of China. J. Geophys.l Res-Biogeo., 124(5): 1148-1170, 2019.

Hu, C., Xu, J., Liu, C., Chen, Y., Yang, D., Huang, W., Deng, L., Liu, S., Griffis, T. J., and Lee, X.: Anthropogenic and natural controls on atmospheric δ13C-CO2 variations in the Yangtze River delta: insights from a carbon isotope modeling framework, Atmos. Chem. Phys., 21, 10015–10037, https://doi.org/10.5194/acp-21-10015-2021, 2021.

Hu, C., Griffis, T.J., Xia, L., Xiao, W., Liu, C., Xiao, Q., Huang, X., Yang, Y., Zhang, L., Hou, B., Anthropogenic CO_2 emission reduction during the COVID-19 pandemic in Nanchang City, China, Environ. Pollut., 309, 119767, doi: https://doi.org/10.1016/j.envpol.2022.119767, 2022.

Huang, W. J., T. J. Griffis, C. Hu, W. Xiao, and X. H. Lee. Seasonal variations of CH_4 emissions in the Yangtze River Delta region of China are driven by agricultural activities. Adv. Atmos. Sci., 38(9), 1537−1551, https://doi.org/10.1007/s00376-021-0383-9, 2021.

Isaksen I S, Gauss M, Myhre G, Anthony W, Katey M and Ruppel C 2011 Strong atmospheric chemistry feedback to climate warming from Arctic methane emissions. Global Biogeochem. Cy. 25 GB2002, 2011.

Kumar, P.; Broquet, G.; Caldow, C.; et al. Near-field atmospheric inversions for the localization and quantification Of controlled methane releases using stationary and mobile measurements. Q. J. R. Meteorol. Soc. 2022, 148, 1886−1912

Kissas K , Ibrom A , Kjeldsen P , et al. Methane emission dynamics from a Danish landfill: The effect of changes in barometric pressure. Waste Management, 2022, 138:234-242.

Lian, J., Bréon, F.-M., Broquet, G., Lauvaux, T., Zheng, B., Ramonet, M., Xueref-Remy, I., Kotthaus, S., Haeffelin, M., and Ciais, P.: Sensitivity to the sources of uncertainties in the modeling of atmospheric CO_2 concentration within and in the vicinity of Paris, Atmos. Chem. Phys., 21, 10707–10726, https://doi.org/10.5194/acp-21-10707-2021, 2021.

Lin, X., Zhang, W., Crippa, M., Peng, S., Han, P., Zeng, N., Yu, L., and Wang, G.: A comparative study of anthropogenic CH_4 emissions over China based on the ensembles of bottom-up inventories, Earth Syst. Sci. Data, 13, 1073–1088, https://doi.org/10.5194/essd-13-1073-2021, 2021.

Lopez-Coto, I., Ren, X., Salmon, O. E., Karion, A., Shepson, P. B., Dickerson, R. R., Stein, A., Prasad, K., and Whetstone, J. R.: Wintertime CO_2, CH_4, and CO Emissions Estimation for the Washington, DC-Baltimore Metropolitan Area Using an Inverse Modeling Technique, Environmental Science and Technology, 54, 2606–2614, https://doi.org/10.1021/acs.est.9b06619, 2020.

Lou, Z., Cai, B.F., Zhu, N., Zhao, Y., Geng, Y., Yu, B., Chen, W., Greenhouse gas emission inventories from waste sector in China during 1949–2013 and its miti- gation potential. J. Clean. Prod. 157, 118–124. https://doi.org/10.1016/j.jclepro. 2017.04.135, 2017.

Lu, X., Jacob, D. J., Zhang, Y., Maasakkers, J. D., Sulprizio, M. P., Shen, L., Qu, Z., Scarpelli, T. R., Nesser, H., Yantosca, R. M., Sheng, J., Andrews, A., Parker, R. J., Boesch, H., Bloom, A. A., and Ma, S.: Global methane budget and trend, 2010–2017: com- plementarity of inverse analyses using in situ (GLOBALVIEW- plus CH4 ObsPack) and satellite (GOSAT) observations, At- mos. Chem. Phys., 21, 4637–4657, https://doi.org/10.5194/acp-21-4637-2021, 2021.

Kaiho K., Koga S. Impacts of a massive release of methane and hydrogen sulfide on oxygen and ozone during the late Permian mass extinction. Global Planetary Change, 107:91-101, https://doi.org/10.1016/j.gloplacha.2013.04.004, 2013.

Maasakkers, J. D., Varon, D. J., Elfarsdóttir, A., McKeever, J., Jervis, D., Mahapatra, G., Pandey, S., Lorente, A., Borsdorff, T., Foorthuis, L. R., Schuit, B. J., Tol, P., van Kempen, T. A., van Hees, R., & Aben, I. Using satellites to uncover large methane emissions from landfills. Sci. Adv. 8, eabn9683, 10. https://doi.org/10.1126/sciadv.abn9683, 2022.

Masuda, S., Sano, I., Hojo, T., Li, Y., Nishimura, O., The comparison of greenhouse gas emissions in sewage treatment plants with different treatment processes. Chemosphere 193, 581–590, 2018.

Miles, N. L., Richardson, S. J., Lauvaux, T., Davis, K. J., Balashov, N. V., Deng, A., Turnbull, J. C., Sweeney, C., Gurney, K. R., Patarasuk, R., Razlivanov, I., Cambaliza, M. O. L. and Shepson, P. B.: Quantification of urban atmospheric boundary layer greenhouse gas dry mole fraction enhancements in the dormant season: Results from the Indianapolis Flux Experiment (INFLUX), Elem Sci Anth, 5, 27, doi:10.1525/elementa.127, 2017.

Miller, S. M., Matross, D. M., Andrews, A. E., Millet, D. B., Longo, M., Gottlieb, E. W., Hirsch, A. I., Gerbig, C., Lin, J. C., Daube, B. C., Hudman, R. C., Dias, P. L. S., Chow, V. Y., and Wofsy, S. C.: Sources of carbon monoxide and formaldehyde in North America determined from high-resolution atmospheric data, Atmos. Chem. Phys., 8, 7673–7696, https://doi.org/10.5194/acp-8-7673-2008, 2008.

Miller, S. M., Michalak, A. M., Detmers, R. G., Hasekamp, O. P., Bruhwiler, L. M. P., & Schwietzke, S. China's coal mine methane regulations have not curbed growing emissions. Nature Communications, 10(1), 303–308. https://doi.org/10.1038/s41467-018-07891-7, 2019.

Mønster, J., Kjeldsen, P. and Scheutz, C. (2019) Methodologies for measuring fugitive methane emissions from landfills – a review. In Waste Management., 87, 835– 859. https://doi.org/10.1016/j.wasman.2018.12.047.

National Bureau of Statistics of China (NBSC), China Statistical Yearbook (China Statistics Press, 2015) (in Chinese).

Pak N M , Heerah S , Zhang J , et al. The Facility Level and Area Methane Emissions inventory for the Greater Toronto Area (FLAME-GTA)[J]. Atmospheric Environment, 2021, 252(9):118319.

Peng, S., Piao, S., Bousquet, P., Ciais, P., Li, B., Lin, X., Tao, S., Wang, Z., Zhang, Y., and Zhou, F.: Inventory of anthropogenic methane emissions in mainland China from 1980 to 2010, Atmos. Chem. Phys., 16, 14545–14562, https://doi.org/10.5194/acp-16-14545-2016, 2016.

Sargent, M., Barrera, Y., Nehrkorn, T., Hutyra, L. R., Gately, C. K., Mckain, K., Sweeney, C., Hegarty, J., Hardiman, B., Steven C. Wofsy, S. C.: Anthropogenic and biogenic CO_2 fluxes in the Boston urban region, P. Natl. Acad. Sci. USA., 115(40), https://doi.org/10.1073/pnas.1803715115, 2018.

Saunois, M., Stavert, A. R., Poulter, B., et al., The Global Methane Budget 2000–2017, Earth Syst. Sci. Data, 12, 1561– 1623, https://doi.org/10.5194/essd-12-1561-2020, 2020.

Seto, K. C. hakal, S. Bigio, A. Blanco, H. elgado, G. C. ewar,. Huang, L. Inaba, A. Kansal, A. Lwasa, S. cahon, J. ller,. B. urakami, J. Nagendra, H. amaswami, A. Humansettlements, infrastructure and spatial planning.Climate Change 2014:Mitigation of Climate Change. IPCC Working Group III Contribution toAR5; Cambridge University Press, 2014; Chapter 12.

Solazzo, E., Crippa, M., Guizzardi, D., Muntean, M., Choulga, M., and Janssens-Maenhout, G.: Uncertainties in the Emissions Database for Global Atmospheric Research (EDGAR) emission inventory of greenhouse gases, Atmos. Chem. Phys., 21, 5655–5683, https://doi.org/10.5194/acp-21-5655-2021, 2021.

Spokas, K.A., et al. 2021. Modeling landfill CH4 emissions: CALMIM international fieldvalidation, using CALMIM to simulate management strategies, current and futureclimate scenarios. Elem Sci Anth, 9: 1. https://doi.org/10.1525/elementa.2020.00050Do, 2020.

Tolaymat, T., M., R. B. Green, G. R. Hater, M. A. Barlaz, P. Black, D. Bronson, J. Powell, Evaluation of landfill gas decay constant for municipal solid waste landfills operated as bioreactors. J. Air Waste Manage. Assoc. 60, 91–97, 2010.

Thoning, K. W., Tans, P. P., and Komhyr, W. D.: Atmospheric carbon dioxide at Mauna Loa observatory 2. Analysis of the NOAA/GMCC data, 1974–1985, J. Geophys. Res.-Atmos., 94, 8549–8565, https://doi.org/10.1029/JD094iD06p08549, 1989.

Tian, J., Gong, Y., Li, Y., Chen, X., Zhang, L., & Sun, Y. (2022). Can policy implementation increase public waste sorting behavior? The comparison between regions with and without waste sorting policy implementation in China. Journal of Cleaner Production, 132401.

United States Environmental Protection Agency (USEPA), Global Mitigation of Non-CO_2 Greenhouse Gases 2010-2030 (United States Environmental Protection Agency Office of Atmospheric Programs (6207J), EPA-430-R-13-011, 2013); www.epa.gov/sites/production/files/2016-07/documents/mac_report_2014-exec_summ.compressed.pdf

Verhulst, K. R., Karion, A., Kim, J., Salameh, P. K., Keeling, R. F., Newman, S., Miller, J., Sloop, C., Pongetti, T., Rao, P., Wong, C., Hopkins, F. M., Yadav, V., Weiss, R. F., Duren, R. M. and Miller, C. E.: Carbon dioxide and methane measurements from the Los Angeles Megacity Carbon Project – Part 1: calibration, urban enhancements, and uncertainty 10 estimates, Atmos. Chem. Phys., 17(13), 8313–8341, doi:10.5194/acp-17-8313-2017, 2017

Wang, X., A. S. Nagpure, J. F. DeCarolis, M. A. Barlaz, Characterization of uncertainty in estimation of methane collection from select U.S. landfills. Environ. Sci. Technol. 49, 1545–1551, 2015.

Wang, Y., Wang, X., Wang, K. *et al.* The size of the land carbon sink in China. *Nature*, E7–E9. https://doi.org/10.1038/s41586-021-04255-y, 2022.

Williams, J. P., Ars, S., Vogel, F., Regehr, A., & Kang, M. (2022). Differentiating and Mitigating Methane Emissions from Fugitive Leaks from Natural Gas Distribution, Historic Landfills, and Manholes in Montréal, Canada. Environmental Science & Technology. https://doi.org/10.1021/acs.est.2c06254

Yadav, V., Duren, R., Mueller, K., Verhulst, K. R., Nehrkorn, T., and Kim, Jet., Spatio-temporally resolved methane fluxes fromthe Los Angeles megacity J. Geophys. Res. Atmos. 124, 5131–5148 (2019).

Zhao, X., Jin, X., Guo, W., Zhang, C., Shan, Y., Du, M., Tillotson, M., Yang, H., Liao, X., and Li, Y.: China's urban methane emissions from municipal wastewater treatment plant, Earths Future, 7, 480–490, 2019.

Zhao, Z., Bian, R., Zhao, F., Chai, X., Implications of municipal solid waste disposal methods in China on greenhouse gas emissions. Renew. Sust. Energ. Rev. 39 (3). https://doi.org/10.1002/ep.13372, 2019.

Zhang, B. and Chen, G.: China's CH_4 and CO_2 emissions: Bottomup estimation and comparative analysis, Ecol. Indic., 47, 112– 122, https://doi.org/10.1016/j.ecolind.2014.01.022, 2014.

Zhang, K., Lee, X., Schultz, N. M., Huang, Q., Liu, Z., Chu, H., Zhao, L., & He, C. A global dataset on subgrid land surface climate (2015-2100) from the Community Earth System Model. Geosci. Data J., 1–12. https://doi.org/10.1002/gdj3.153, 2022.

Zhang Y., Fang S., Chen J., Lin Y., Chen Y., Liang R., Jiang K., Parker R., Boesch H., Steinbacher M., Sheng J., Lu X., Shaojie Song, Shushi Peng: Observed Changes in China's Methane Emissions Linked to Policy Drivers, Proceedings of the National Academy of Sciences, 119, e2202742119, 2022.

Zhejiang Provincial Bureau of Statistics, Survey Office of the National Bureau of Statistics in Zhejiang, Zhejiang Statistical Yearbook 2018-2019 (China Statistics Press, Beijing, China, 2019)

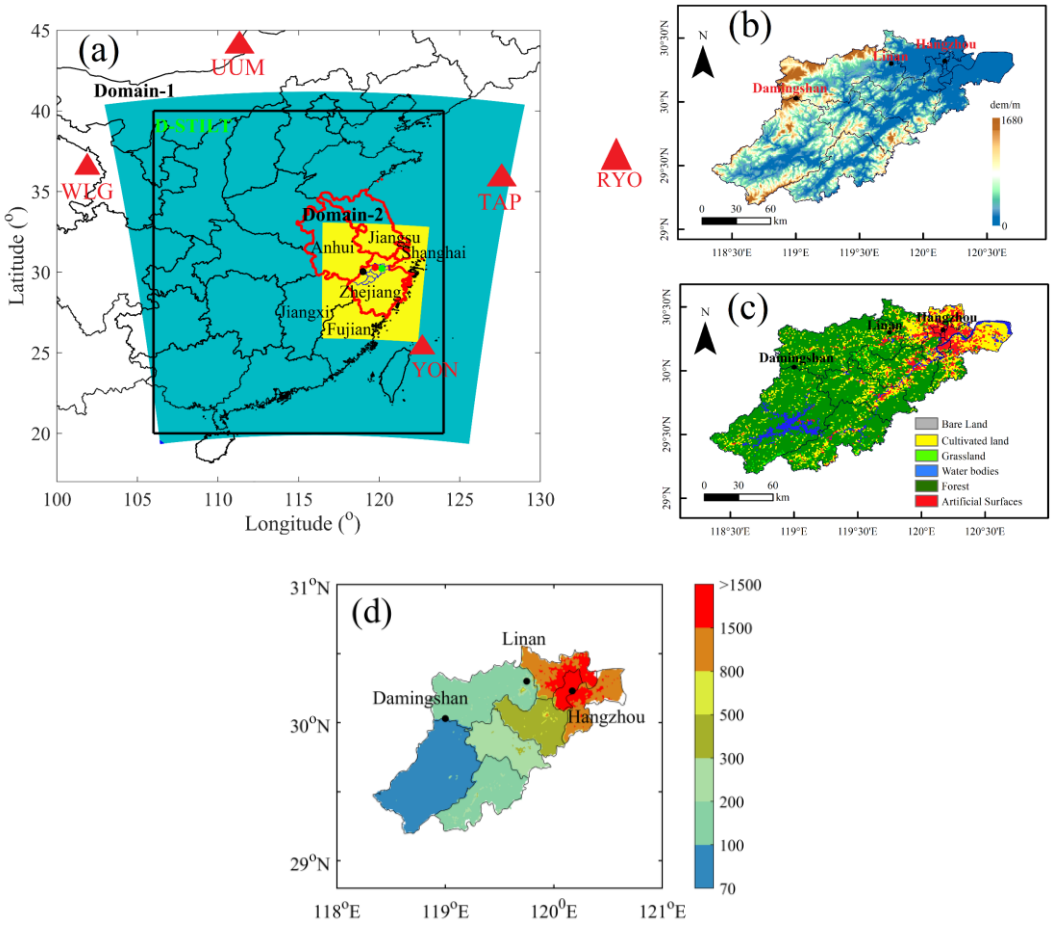

Figure 1. (a) WRF-STILT model domain setups, three CH_4 concentration observation sites in Hangzhou city, and five CH_4 background sites, note the green, red and black dots represent locations for Hangzhou site, Linan site and Damingshan site, respectively, Yangtze River Delta regions is displayed in red boundary, back rectangle represents domain in STILT model, (b) geophysical height within Hangzhou city, (c) land surface categories in Hangzhou city, and (d) population density in Hangzhou city for year 2019, units: person per km^2.

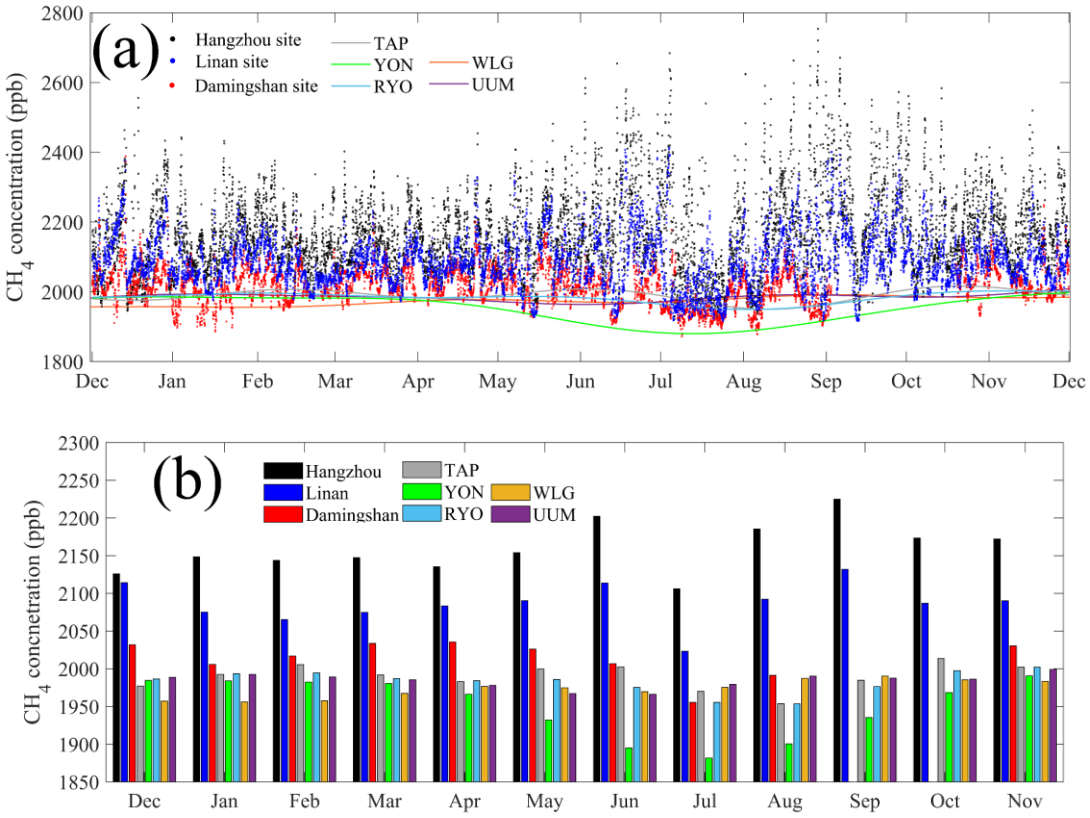

Figure 2. (a) Hourly CH_4 concentrations at three sites within Hangzhou city as Hangzhou site, Linan site, and Damingshan site, and fitting CH_4 background based on CCGCRV regression method at five background sites as TAP, YON, RYO, WLG and UUM, (b) monthly mean of CH_4 concentrations for above eight sites. Note the CH_4 background is smoothed by using CCGCRV fitting method on weekly or hourly observations, which can filter large fluctuations caused by sudden and unidentified sources

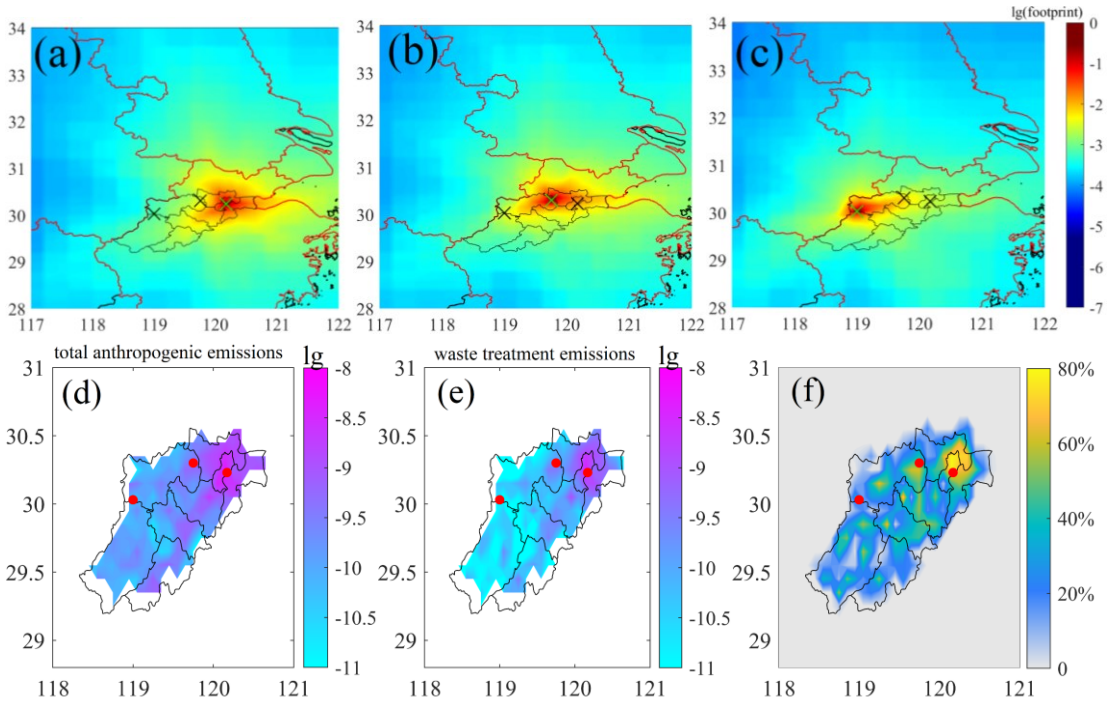

Figure 3. Annual averages of simulated footprint for (a) Hangzhou site, (b) Linan site, and (c) Damingshan site, where the green symbol "×" indicates receptor location in each pannel, (d) total anthropogenic CH_4 emissions in EDGAR v6.0 inventory, (e) waste treatment CH_4 emissions in EDGAR v6.0 inventory, and (f) proportions of waste treatment to total anthropogenic CH_4 emissions, red dot represents three sites, units for footprint: ppm m^2 s mol^{-1}, units for emissions: kg m^{-2} s^{-1}. The divisions in Hangzhou city are different districts.

1007

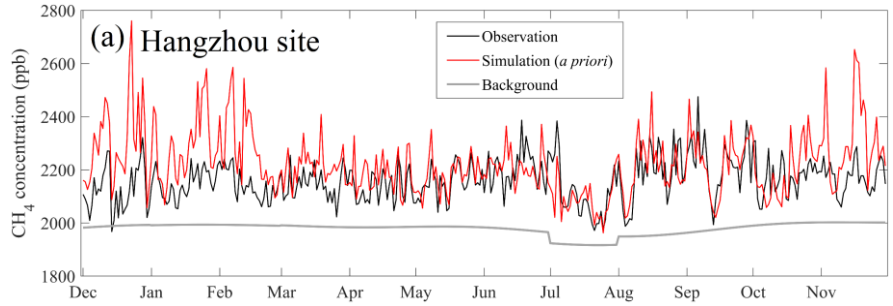

1008

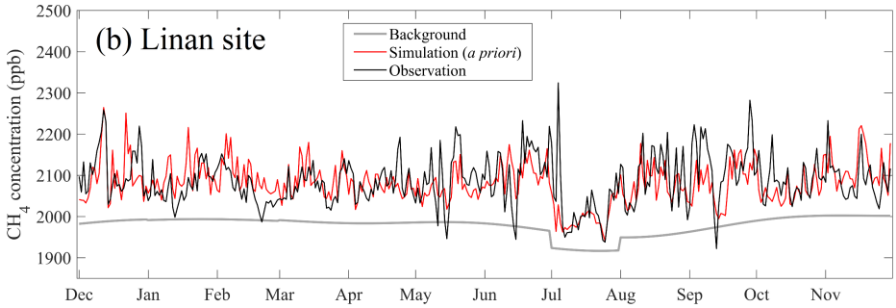

1009

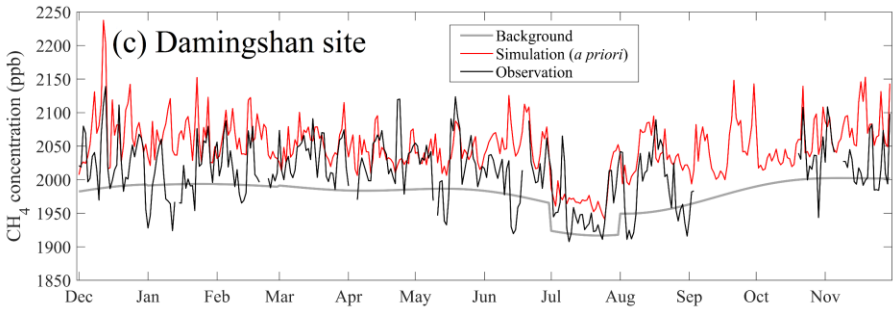

1010

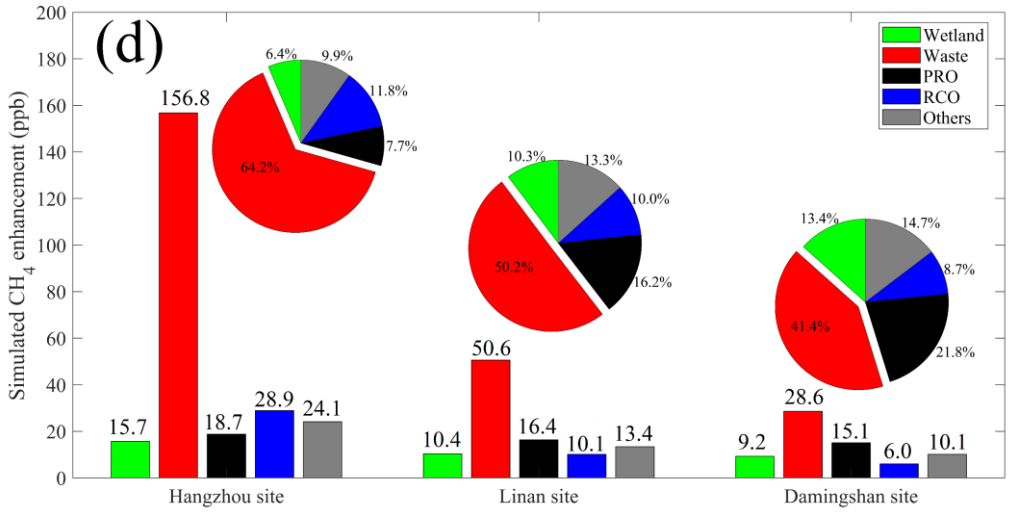

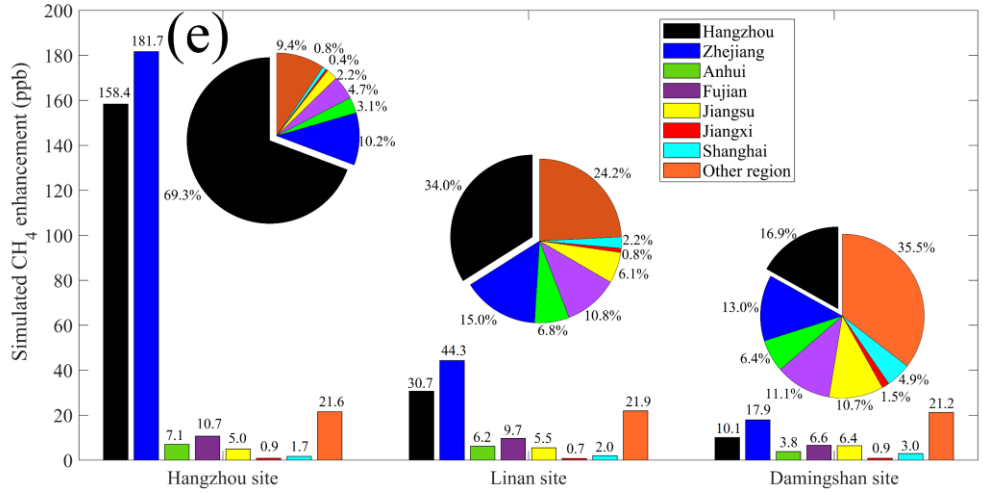

Figure 4. Comparisons between daily CH_4 observations and simulations for (a) Hangzhou site, (b) Linan site, (c) Damingshan site, (d) simulated CH_4 enhancements from main emission categories (e) simulated anthropogenic CH_4 enhancement from different regions and its proportions. Note the blue color for the bar charts include all contributions from "Zhejiang", including "Hangzhou"; and the blue regions in the pie charts represent rest regions of "Zhejiang minus Hangzhou".

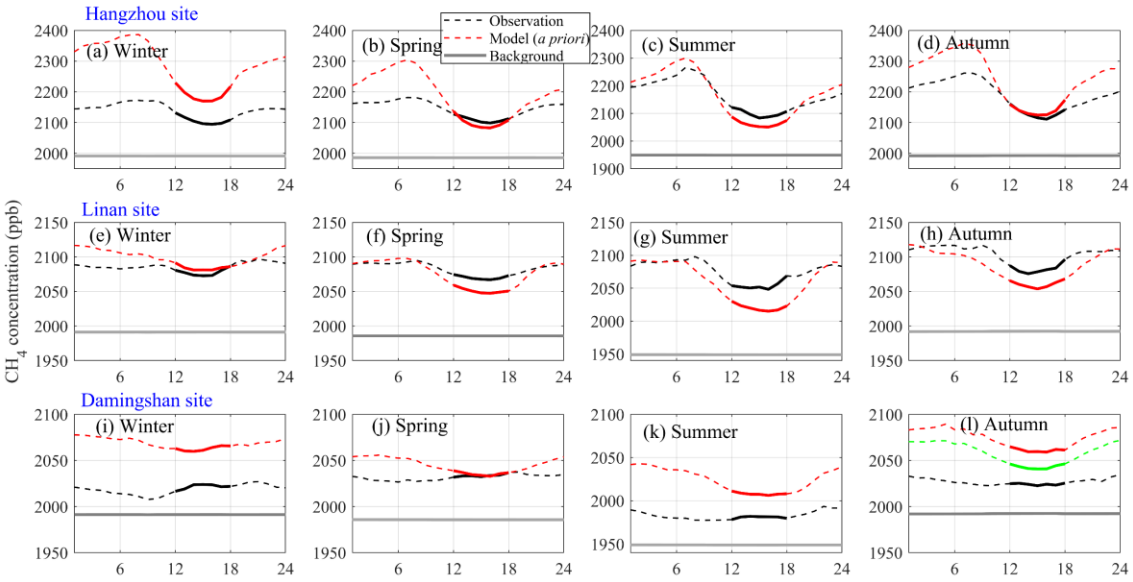

Figure 5. Seasonal averaged diurnal variations for Hangzhou site in (a) winter, (b) spring, (c) summer, (d) autumn, and Linan site in (e) winter, (f) spring, (g) summer, (h) autumn, and Damingshan site in (i) winter, (j) spring, (k) summer, (l) autumn; Note because of two months of data gap in Autumn for Damingshan site, the green line is for all September-November simulations, red line only represent simulation of corresponding period for available observation data, and bold lines represents data between 12:00 and 18:00.

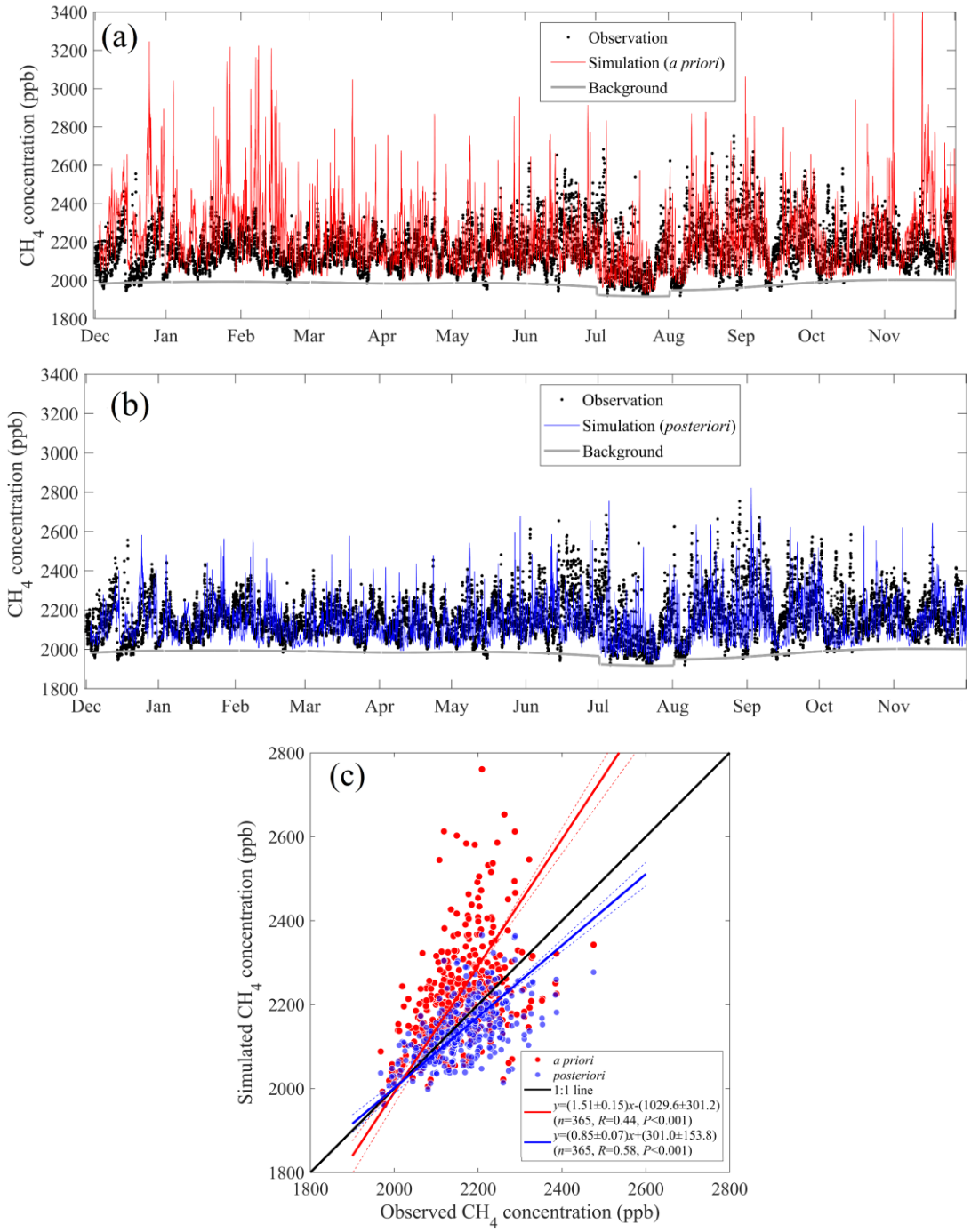

Figure 6. Comparisons of hourly CH_4 concentrations at Hangzhou site between observations and simulations by using (a) *a priori* and (b) *posteriori* emissions, (c) scatter plots of daily CH_4 averages by using *a priori* and *posteriori* emissions.

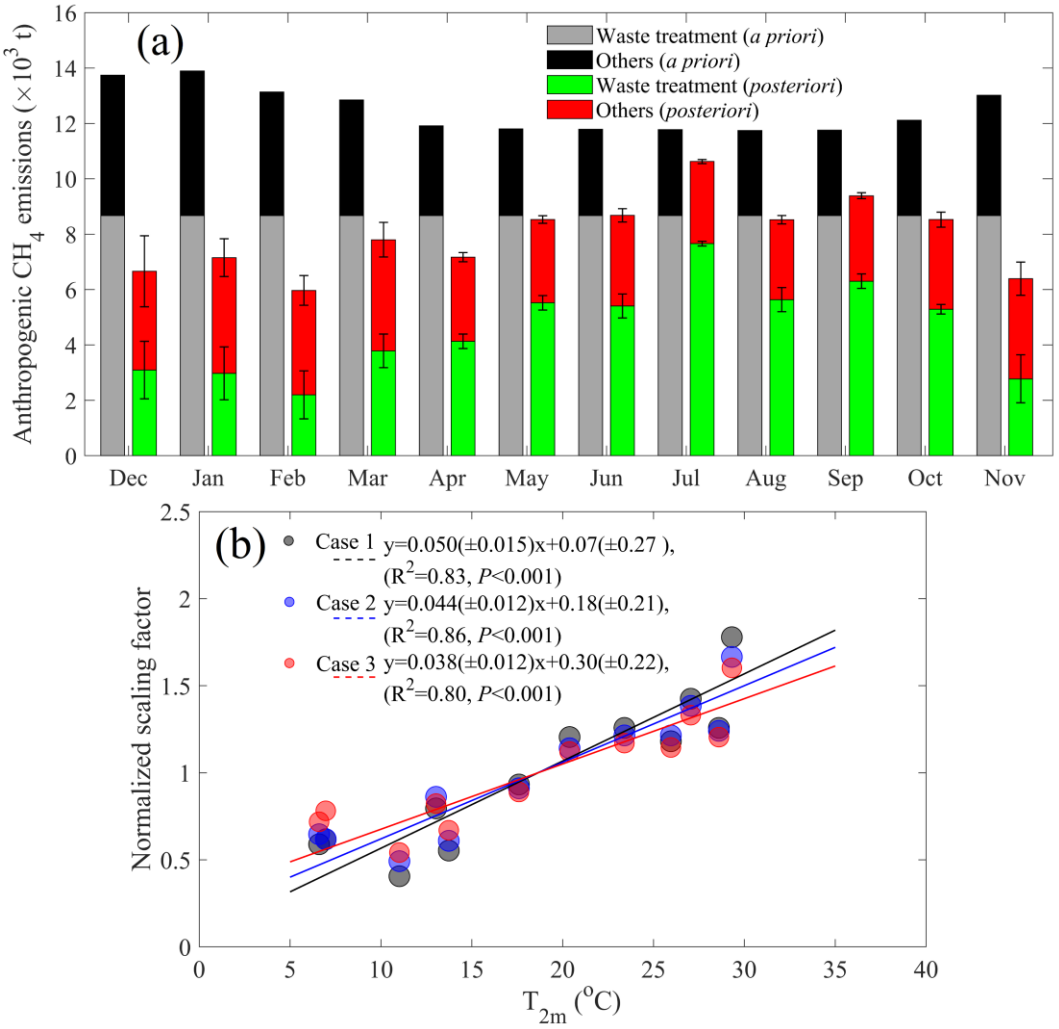

Figure 7. (a) Monthly anthropogenic (excluding agricultural soil) CH_4 emissions for *a priori* and *posteriori* emissions for Hangzhou city, (b) relationship between the monthly *posteriori* CH_4 emissions and temperature in three cases.

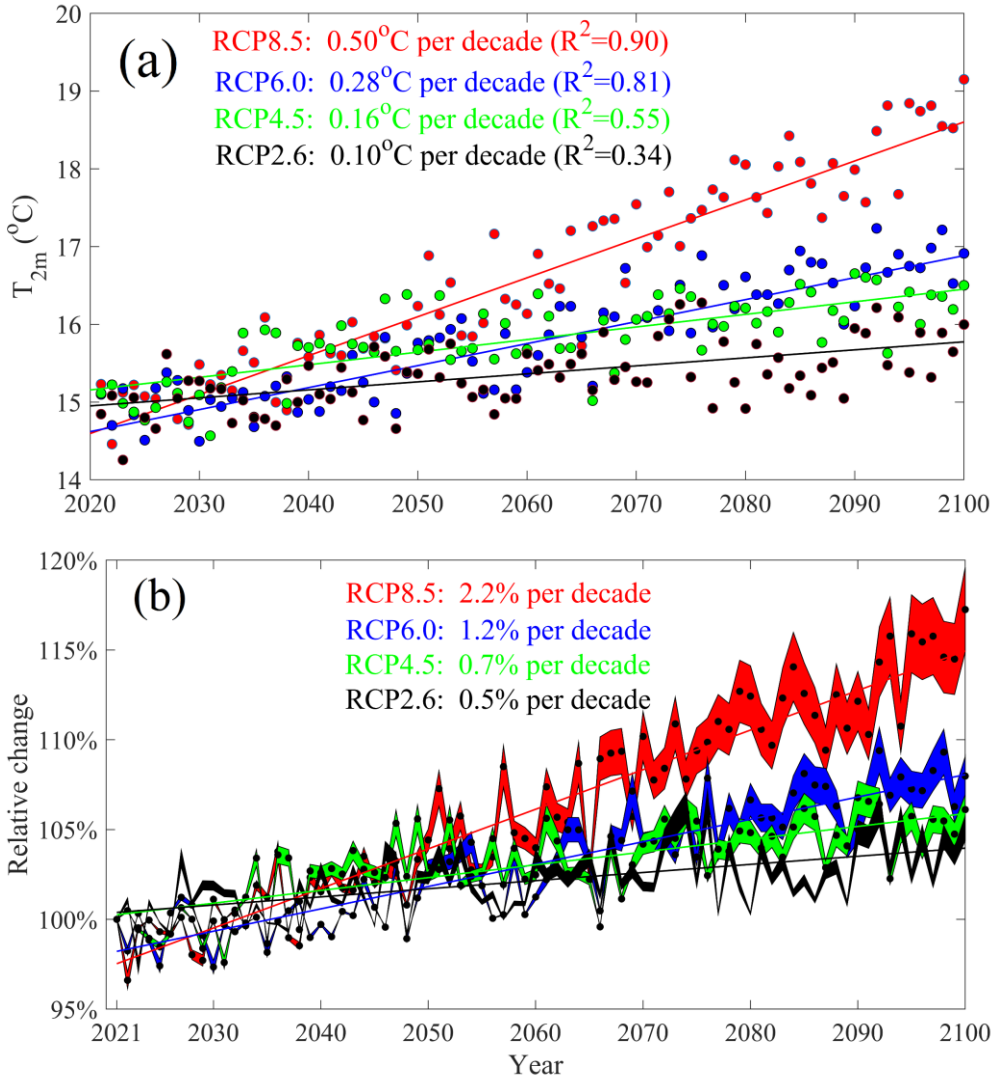

Figure 8. (a) Annual air temperature from year 2021 to 2100 for four different global warming scenarios for Hangzhou city, (b) the projected relative change of waste treatment CH_4 emissions (or EFs) for Hangzhou city, note the shading indicates extent of three cases.

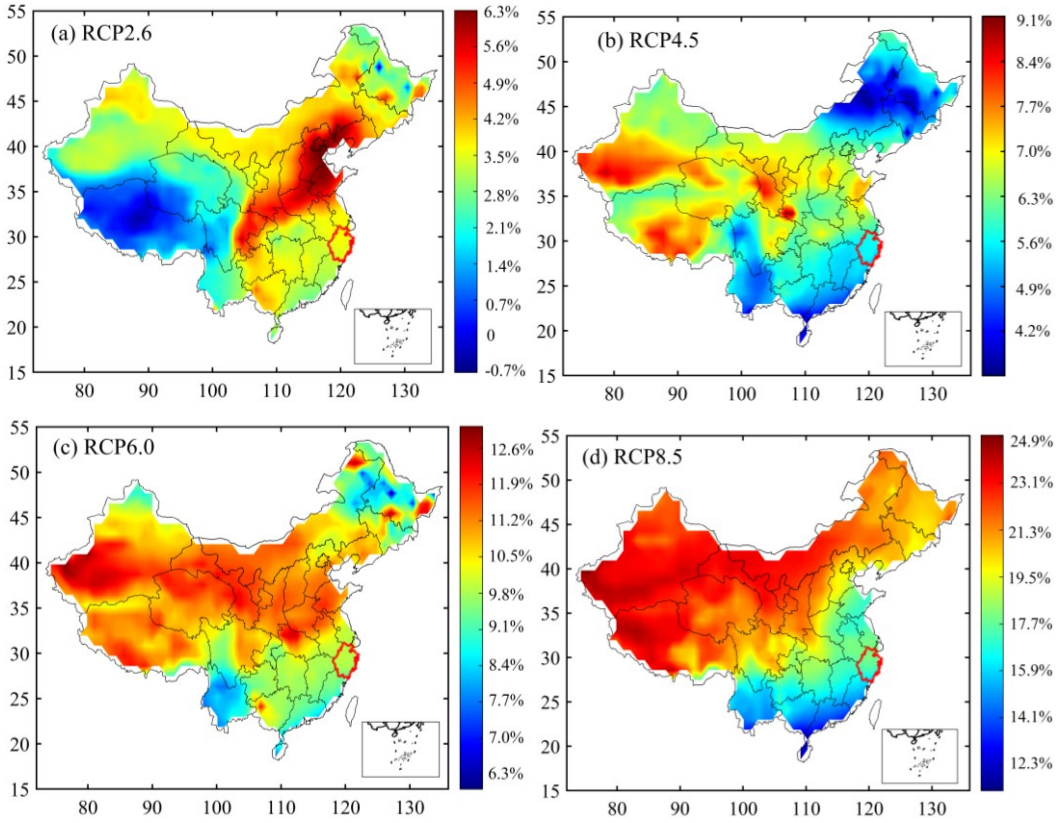

Figure 9. Global warming induced relative changes of waste treatment CH_4 EFs by year of 2100 for (a) RCP2.6, (b) RCP4.5, (c) RCP6.0, and (d) RCP8.5 scenarios. Note the red boundary is Zhejiang province.

Table 1. The *posteriori* SFs for different categories in three cases, where wetland: natural and agricultural wetland, Waste: waste treatment, PRO: fuel exploitation, RCO: energy for building, Others: the rest anthropogenic emissions.

	Case 1			Case 2					Case 3		
Month	Wetland	Waste	Others	Wetland	Waste	PRO	RCO	Others	Wetland	Waste	Others
1	1.00	0.29	0.83	1.00	0.34	0.90	0.80	0.93	1.00	0.40	0.72
2	1.00	0.20	0.89	1.00	0.26	0.97	0.83	0.93	1.00	0.30	0.77
3	1.03	0.39	1.04	1.02	0.46	1.07	0.80	0.97	1.02	0.46	0.95
4	1.10	0.46	0.96	1.08	0.48	1.01	0.95	0.93	1.08	0.49	0.91
5	1.12	0.62	0.99	1.10	0.64	1.06	0.97	0.92	1.11	0.65	0.95
6	1.22	0.59	1.09	1.18	0.64	1.05	0.97	1.03	1.18	0.64	1.05
7	1.10	0.88	0.96	1.09	0.88	1.00	1.00	0.94	1.09	0.89	0.94
8	1.05	0.62	0.95	1.01	0.66	0.99	0.97	0.95	1.01	0.67	0.91
9	1.04	0.71	1.01	1.02	0.73	0.96	0.98	1.04	1.02	0.74	0.98
10	1.06	0.60	0.94	1.06	0.61	0.92	0.96	1.00	1.06	0.62	0.90
11	1.01	0.27	0.86	1.00	0.32	0.91	0.85	0.93	1.00	0.37	0.75
12	1.00	0.31	0.70	1.00	0.33	0.75	0.79	0.91	1.00	0.43	0.58